The Ionospheric response During 2013 Stratospheric Sudden Warming over East Asia Region

Wang fei fei[1], Shan xin jian[2], Li Na[1], Zhang hong bo[3], Sheng dong sheng[3], Sun shu ji[3], Xu tong[3], and Tang ji[2]

[1]Information center China Research Institute of Radiowave Propagation
[2]Institute of Geology China Earthquake Administration
[3]CETC

November 26, 2022

Abstract

Ionospheric response to sudden stratospheric warming (SSW) are not well understood. During the 2013 SSW, ionospheric disturbances were observed in eighteen stations on three meridional chains of 100°E, 110°E and 120°E ranging from 19.03°N to 49.21°N at latitudes over East Asia region. The TEC response showed evident semi-diurnal disturbance that enhancement in the morning and depletion in the afternoon. The maximum TEC increased by more than 220% on the chain 120°E. In addition, the semi-diurnal disturbance of TEC were enhanced and indicated evident latitudinal and longitudinal dependence. The wavelet spectra of semi-diurnal disturbance in TEC presented quasi-16 day planetary wave-like oscillations at middle latitudes and quasi-10 day planetary wave-like oscillations at low latitudes. Meanwhile, the zonal winds and meridional winds at altitudes of 92-100 km showed quasi-16 day planetary wave at Mohe located middle latitude and quasi-10 day planetary wave at Sanya located low latitude, which are agree with semi-diurnal disturbance of TEC. Especially, the 12-hour component of TEC showed a quasi-16 day periodic component at middle latitude and a quasi-10 day periodic component at low latitude, indicating that the modulated semi-diurnal tides may transmit these 10 day and 16 day planetary wave-like oscillations to the ionosphere. The coupling between the atmosphere and ionosphere may be strengthened by the quasi-16 day waves at middle latitude and quasi-10 day waves at low latitude. This can further confirm the PW-tide interaction theory during the 2013 SSW and it is of significance in the middle and low latitude ionospheric response to SSW.

The Ionospheric response During 2013 Stratospheric Sudden Warming over East Asia Region

Feifei Wang[1,2], Ji Tang[1], Xinjian Shan[1], Na Li[2], Hongbo Zhang[2],Dongsheng Sheng[2], Shuji Sun[2], Tong Xu[2]

Institute of Geology China Earthquake Administration

Information center China Research Institute of Radiowave Propagation Qingdao, China

Abstract

Ionospheric response to sudden stratospheric warming (SSW) are not well understood. During the 2013 SSW, ionospheric disturbances were observed in eighteen stations on three meridional chains of 100°E, 110°E and 120°E ranging from 19.03°N to 49.21°N at latitudes over East Asia region. The TEC response showed evident semi-diurnal disturbance that enhancement in the morning and depletion in the afternoon. The maximum TEC increased by more than 220% on the chain 120°E. In addition, the semi-diurnal disturbance of TEC were enhanced and indicated evident latitudinal and longitudinal dependence. The wavelet spectra of semi-diurnal disturbance in TEC presented quasi-16 day planetary wave-like oscillations at middle latitudes and quasi-10 day planetary wave-like oscillations at low latitudes. Meanwhile, the zonal winds and meridional winds at altitudes of 92-100 km showed quasi-16 day planetary wave at Mohe located middle latitude and

quasi-10 day planetary wave at Sanya located low latitude, which are agree with semi-diurnal disturbance of TEC. Especially, the 12-hour component of TEC showed a quasi-16 day periodic component at middle latitude and a quasi-10 day periodic component at low latitude, indicating that the modulated semi-diurnal tides may transmit these 10 day and 16 day planetary wave-like oscillations to the ionosphere. The coupling between the atmosphere and ionosphere may be strengthened by the quasi-16 day waves at middle latitude and quasi-10 day waves at low latitude. This can further confirm the PW-tide interaction theory during the 2013 SSW and it is of significance in the middle and low latitude ionospheric response to SSW.

Key words: Ionosphere, SSW, MLT

Introduction

Stratospheric Sudden Warming (SSW) events are large-scale meteorological phenomena that usually occur in the Northern Hemisphere from December to February. SSWs are characterized by a rapid increase in the polar stratospheric temperature by several tens of degrees with a weakening or reversal of eastward zonal mean zonal winds. They result from the breaking of upward propagating stationary planetary waves (SPWs) from the troposphere to the stratosphere. These amplified SPWs interact with the stratospheric zonal mean flow and deposit their momentum in westward direction, resulting in an induced mean meridional circulation, which leads to a downwelling in the polar region and increases the temperature due to adiabatic heating (Matsuno, 1971; Hohon, 1980).

The ionized layer of the terrestrial atmosphere from ˜90 to 1000 km above sea level called ionosphere which is mainly influenced by solar and geomagnetic activity. Apart from them, it has been more or less established during the last two decades that lower atmospheric wave processes also perturb the ionosphere significantly, accounting for ˜20% of ionospheric variationss on average (Forbes, 2010), such as planetary wave, tide, gravity wave and so on. During the SSW, the tide may be modulated due to the planetary wave development, temperature and wind, which plays an important role in ionospheric response, and also provides a possible way to study the coupling between the Mesosphere and Lower Thermosphere(MLT) and ionosphere. As a result of SSWs, the ionospheric response is shown in Es layer and F layer in general. The response of Es layer during SSW is mainly focus on Es critical frequency (foEs) due to the PW and tide (Wang, 2015; Korenkova, 2015).

The ionospheric F region is shown to vary in terms of an anomalous daytime semi-diurnal signature in vertical plasma drift(Maute,2015; Goncharenko, 2013), total electron content (TEC)(Liu, 2019; Geetashree, 2020), perturbations in electric fields(Sripathi, 2012), electron and neutral densities, electron and ion temperature, F layer parameters(Chen, 2016;Pancheva, 2011)and the equatorial ionization anomaly (EIA) crest (Upadhayaya, 2013; Qiong, 2020). In addition, previous studies have showed the ionospheric response with latitude or longitude. Geetashree(2020) showed the latitudinal and longitudinal dependence in ionosphere during 2009 and 2013 SSW along the two meridional chains of 10degE and 95degE. Though the coupling mechanism of MLT region and ionospheric response during SSW is not clear, many researchers tried to explained by the neutral wind field,electric field, PW, tide, even gravity waves(GW)(Laskar, 2014; Jonah, 2014).

Jonah(2014) studied the ionospheric response to the 2013 SSW in Brazilian sector using GPS TEC, geomagnetic data and Meteor Radar data. They found that the amplification of the 13-16 day period in TEC during the SSW and simultaneous amplification in zonal and meridional wind components in MLT region. Sripath(2012) analyzed the ionospheric TEC and EEJ effects during 2006 SSW, and found the quasi 16-day planetary waves modulate the tide. Chen(2019) studied the coupling process ionosphere and lower atmosphere during 2013 SSW using the foF2, hmF2 and Wuhan meteor radar data, and explained the ionospheric response through the theory of quasi 16-day planetary waves modulating tide at middle latitude.

However, only a few studies reported the association of the quasi-10-day PWs with SSW events. Matthias(2012) found that the quasi 10-day PWs and quasi 16-days waves were enhanced before and after the polar vortex breakdown with a composite analysis during SSW events in 2004, 2006, 2009, and 2010. Yamazaki (2019) reported slight enhancements of quasi-10-day PWs during some SSW events using the geopotential height data from 2004 to 2018. Luo(2021) showed that the quasi 10-day wave were increased during 2018 SSW at middle latitude.

In this study, we present the latitudinal and longitudinal dependence of the TEC response in East Asia region and the variations of wind in MLT region at middle and low latitudes during the 2013 SSW to further confirm the coupling mechanism by the theory of PW-tide modulation. In section 2 we introduce the data used in this paper, such as GPS TEC, wind, MLS temperature. In section 3 we present the variationss and 12-hour component of TEC and PWs in MLT before they are analyzed and discussed in section 4. Final conclusion are given in section 5.

Data

GPS TEC data

To study the ionospheric response to the major SSW, we used ground-based Global Positioning System (GPS)-derived vertical total electron content (TEC) for selected eighteen stations of Crustal Movement Observation Network of China(CMONC). These stations distribute along the meridional chains of 100degE、110°E and 120°E. Each chain consists of six stations covering varied latitudes from ~19.03°N to ~49.21°N. Table 1 shows the list of GPS stations. The KrigingKalman filter was used to resolve hardware delay and calculate vertical TEC (1TECU=1016) at 30-second intervals(LIU, 2021). We averaged the TEC 30-second intervals to 1-hour in units of TECu (1TECu = 10^{16} electrons/m) in the following.

Table1 List of GPS stations

Sitename	**Longitude/°E**	**latitude/°N**	**Sitename**	**Longitude/°E**	**latitude/°N**
NMEJ	101.06	41.96	nmer	119.77	49.21
QHGC	100.14	37.33	jlcl	123.52	44.55
scgz	100.02	31.61	lnyk	122.61	40.69
ynzd	99.70	27.82	sdrc	122.42	37.17
ynlc	100.08	23.87	jsnt	120.89	31.95
ynmh	100.45	21.95	zjwz	120.76	27.93
nmbt	110.02	40.60	hnmy	109.8	27.88
snak	108.77	32.79	gdzj	110.31	21.16
hbes	109.49	30.28	qion	109.85	19.03

Meteor radar data

The zonal and meridional winds of meteor radar are from the World Data System (WDS) (*http://wdc.geophys.cn/*) to show the variations of planetary waves(PWs) in MLT region. We chose Mohe(122.3°E, 53.5°N) and Sanya(109.6°E, 18.3°N) meteor radars located middle and low latitudes, respectively. The average wind velocities were calculated from the meteor detection results by a least square fitting procedure embedded in the meteor radar software. The height coverage is from 70km to 110km, with the temporal and spatial resolutions are 1hour and 2km, respectively. Figure1 shows the map of GPS stations and Meteor radars used in this paper. GPS receiver stations are green circles, and Meteor radars are red diamonds.

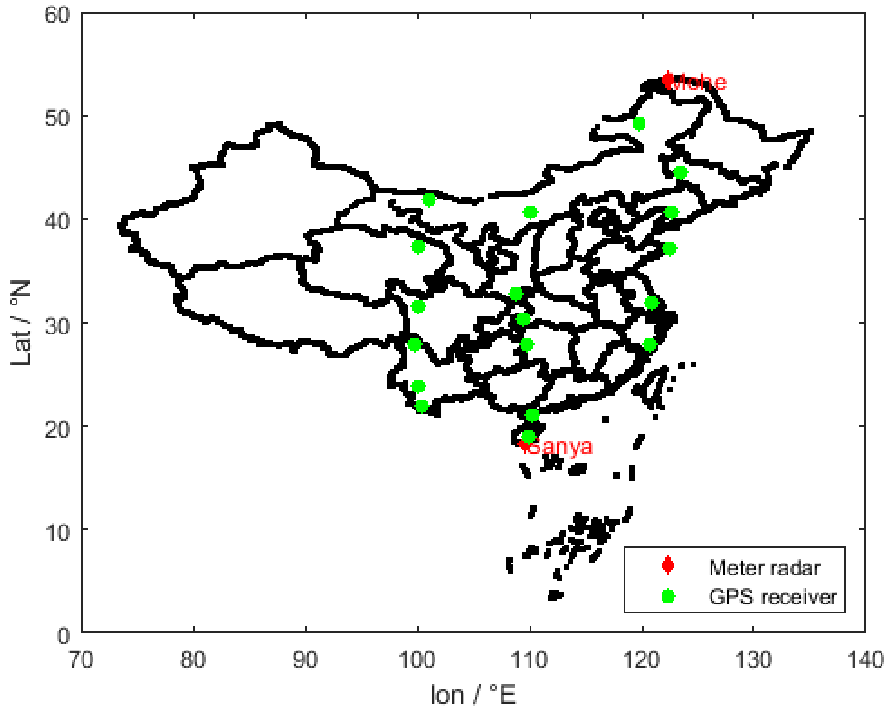

Figure1. The map of GPS receivers and Meteor radars.The green circles represent GPS receiver stations, and red diamonds represent the Meteor radars.

NCEP/NCAR Reanalysis data and Aura MLS data

The National Centers for Environmental Prediction(NCEP) and National Center for Atmospheric Research(NCAR) have cooperated in a project called reanalysis data that the temperature and wind are recovered from land surface, ship, rawinsonde, pilot balloon, aircraft, satellite, and other data (*https://www.psl.noaa.gov//data/gridded/data.ncep.reanalysis.html*). Daily averaged data are 2.5° × 2.5° grid for the whole world in latitude-longitude, 17 pressure levels from the Earth's surface up to 10 hPa. In this study, the stratospheric temperature at 10 hPa (approximately 30 km) at 60° N were used to obtain the temperature anomaly during 2013 SSW.

The Aura satellite was launched in July 2004. The angle between orbital plane and earth's equatorial plane is 82°, it rounds the earth 15 times a day. MLS(Microwave Limb Sounder, MLS) records atmospheric temperatures, density at different isobaric surfaces, 55 isobaric surfaces totally, corresponding height is 12~94km approximately (*https://avdc.gsfc.nasa.gov/pub/data/satellite/Aura/MLS/V04/L2GP/Temperature/*). In this paper, we used the MLS temperature data from December 1, 2012 to February 28, 2013 in the Northern Hemisphere to obtain the variations in temperature.

Results

2012-2013 SSW

Figure2a-d show the temperatures, wind, Kp and F10.7 from December 1, 2012 to February 28, 2013. The stratospheric warming began on the first day of 2013 (January 1, 2013) from ~60km and gradually downward to ~45km, it reached a secondary peak on the fourth day(January 4, 2013), the temperature peak occurred on the twelfth day(January 12, 2013) and the zonal wind shifted from west to east, then the temperature recovered slowly. The solar and geomagnetic conditions are indicated by F10.7 and Kp indices, respectively, both available at the website*http://omniweb.gsfc.nasa.gov/form/dx1.html* . The F10.7 index is in Solar Flux Unit

(SFU = 10-22W/m2 /Hz). In this study, Kp[?]4 is considered geomagnetically quiet. During the 2013 SSW period, geomagnetic activity was quiet, kp index was not more than 4. F10.7 began to increase from January 2013, reaching the peak on January 10, F10.7=168. It's obvious that the solar activity was high during the 2013 SSW.

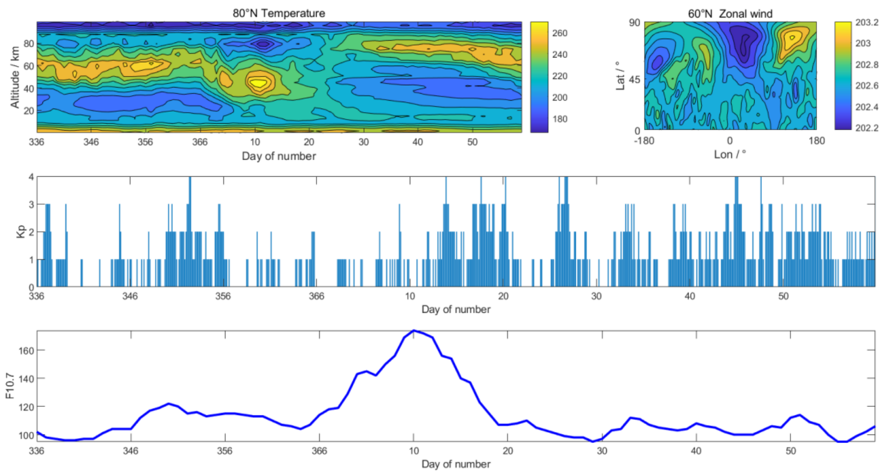

Figure2. The plots of temperatures, wind, F10.7 and Kp from December 1, 2012 to February 28, 2013. a) 80°N zonal averaged temperature. b) 60°N 10hpa zonal averaged wind on January 12. c) kp. d) F10.7.

Ionospheric response

To obtain the latitudinal and longitudinal differences in TEC during 2013 SSW , we chose eighteen GPS stations located along 100°E、110°E and 120°E covering 19.03°N to 49.21°N at latitude. The DTEC is the difference between the observed value(TEC) and the background value(TEC_{med}), which is used to extract the ionospheric disturbance. The background value TEC_{med} is the median value of TEC between December 1, 2012 and December 15, 2012.

Figure3 shows the variations of DTEC from January 1, 2013 to January 31, 2013, the two black dotted lines represent the peak time of the first temperature peak time (January 6) and the second peak time (January 12) , respectively. We can see that the TEC enhancement at ~01:00-08:00(UT) and decrease at ~8:00-12:00(UT) everyday at all stations along the chain 100°E during January 4 to 17, 2013. In other words, enhancement in TEC during morning and early afternoon, and decrease in the afternoon. This TEC semi-diurnal disturbance becomes more and more obvious with decrease in latitude until the YNZD station (latitude: 27.82N), then the semi-diurnal disturbance weaken gradually at YNLC(latitude, 23.87°N) and YNMH(latitude, 21.95°N). The maximum and minimum deviation in TEC are 175% and -58% along the chain 100°E. The variations of TEC on the chain 110°E are similar to the chain 100°E. The TEC semi-diurnal disturbance increase with decrease in latitude until HNMY(latitude, 27.88°N). Meanwhile, GDZJ (latitude, 21.16°N) and QION(latitude, 19.03°N) located in low latitude both weaken. The maximum and minimum deviation in TEC are 150% and -53% of the chain 110°E. On the chain 120°E,the variations of TEC are not clear at NMER(latitude, 49.21degN)and JLCL(latitude, 44.55degN)stations located at higher latitudes. The enhancement in TEC at morning is obvious from LNYK(latitude, 40.69degN) station and to the south until ZJWZ(latitude, 27.93degN) station, and the maximum deviation is 222%. But the decrease in TEC at afternoon is not clearly observed which is coincident with Chen(2019) along the chain 120degE .

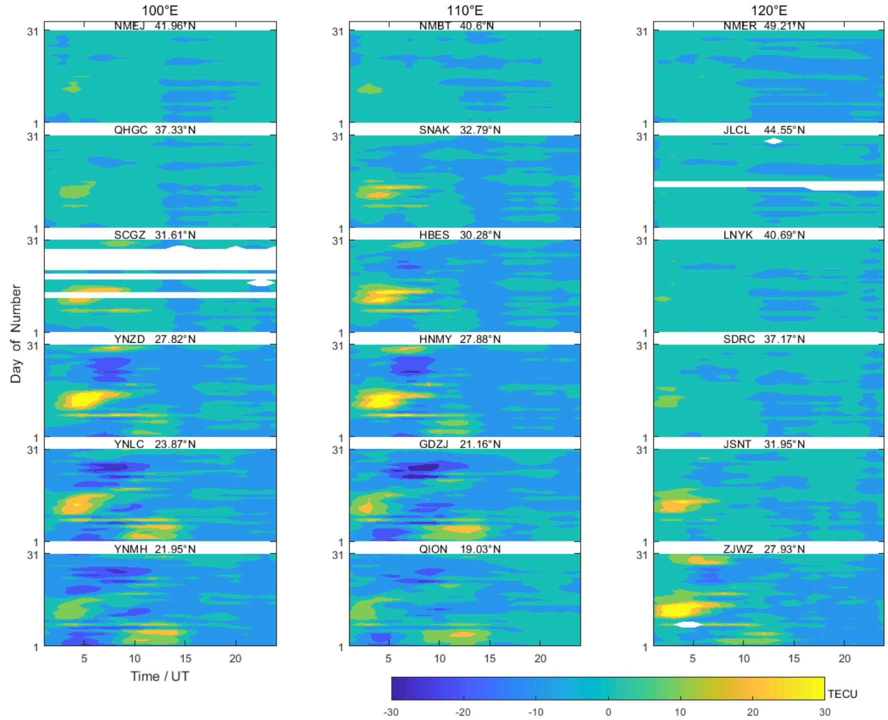

Figure3. variations of DTEC in TECu from January 1 to 31, 2013. The two black dotted lines represent the peak time of the first temperature peak (January 6) and the second peak time (January 12) , respectively.

From the above results, we can see that the TEC variations are not obvious when the latitude greater than 40°N. Inversely, the variations of TEC is obvious significantly with the decrease of latitude. The semi-diurnal variations of TEC in the form of morning enhancement and afternoon depletion are observed along the chain 100°E and 110°E and they increase with the decrease of latitude until ˜27.82°N, then weaken significantly at YNLC, YNMH, GDZJ and QION stations located at latitudes less than 23.87°N. The TEC enhancement in the morning along the chain 120°E is evident, but weakening in the afternoon is not obvious. In a word, the TEC variations shows latitudinal dependence that the semi-diurnal variations in TEC takes equatorial ionization anomaly crest as the dividing line and weakens towards the two poles. Meanwhile, the longitudinal dependence in TEC variations is prominent during 2013 SSW. The TEC variations on the chain 100°E and 110°E are similar but different from the chain 120°E. The maximum deviation of TEC along the chain 120°E is larger than 100°E and 110°E, but the decrease at afternoon is not observed.

12-hour component of TEC

The TEC semi-diurnal disturbance is evident with latitude in sector 3.2. Figure 4 shows the wavelet power spectra of DTEC between January 1 to 31, 2013 to further analyze DTEC periodic variations. It can be seen that the DTEC have prominent 12-hour component period and the latitudinal characteristic is coincident with DTEC variations shown in Figure3. Hence, both DTEC and 12-hour component of DTEC take the equatorial ionization anomaly crest as the dividing line, decrease toward the two poles gradually, and disappear at higher latitude finally. As we all know that the tides occur mainly in MLT region and have maximum amplitudes in this region, they can affect the middle and low latitude ionosphere by modulating E-layer generators. It is assumed that the TEC semi-diurnal disturbance is caused by the semi-diurnal tide enhancement at the middle and low latitudes during 2013 SSW.

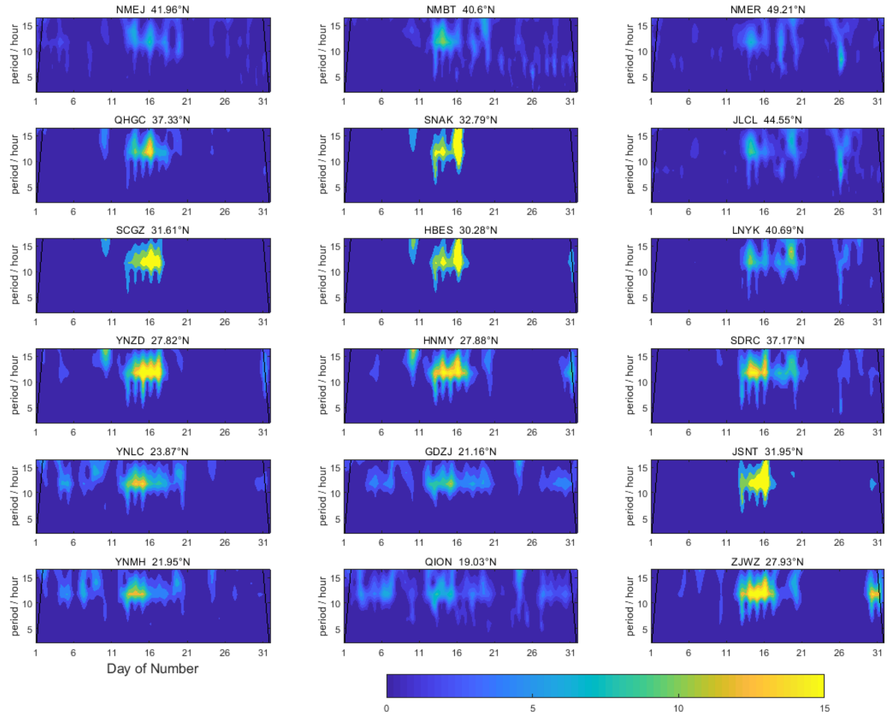

Figure4. Wavelet power spectra of DTEC between January 1 to 31, 2013.

Planetary wave variations in MLT

The zonal and meridional winds of Mohe and Sanya meteor radars were used to analyze the Planetary waves(PWs) variations in MLT region during the 2013 SSW at middle and low latitudes, respectively. The two radars can observe meridional and zonal winds at an altitude from 70km to 110km, with a altitude resolution of 2km and a time resolution of 1h. Considering the data quality, only the wind data at 92km, 96km and 100km heights were selected and processed the time resolution from 1h to 24h. Figure5-6 show the zonal and meridional winds wavelet power spectra at the 92km, 96km and 100km of Mohe and Sanya station, respectively. The quasi 10-Day planetary wave amplitudes are enhanced in zonal wind at Mohe all altitudes from December 20, 2012 to January 10, 2013 before warming, and the maximum amplitude is 7m/s at 92km. Quasi-16-day planetary wave amplitudes are enhanced in meridional wind from December 11, 2012 to January 27, 2013, and the maximum amplitude is 13.4m/s. Hence the quasi 16-day wave amplitude is higher than quasi 10-day wave amplitude at Mohe station. At Sanya, quasi-10-day planetary wave amplitudes are increased at all altitudes except for the 92km zonal wind, and the maximum amplitude is 7m/s. In general, the qusai-16-day waves are enhanced mainly at Mohe located at middle latitude and the qusai-10-day waves mainly at Sanya located at low latitude which are consistent with the variations of quasi-10-day and quasi-16-day planetary waves during SFW event in 2015 analyzed by Yu(2019).

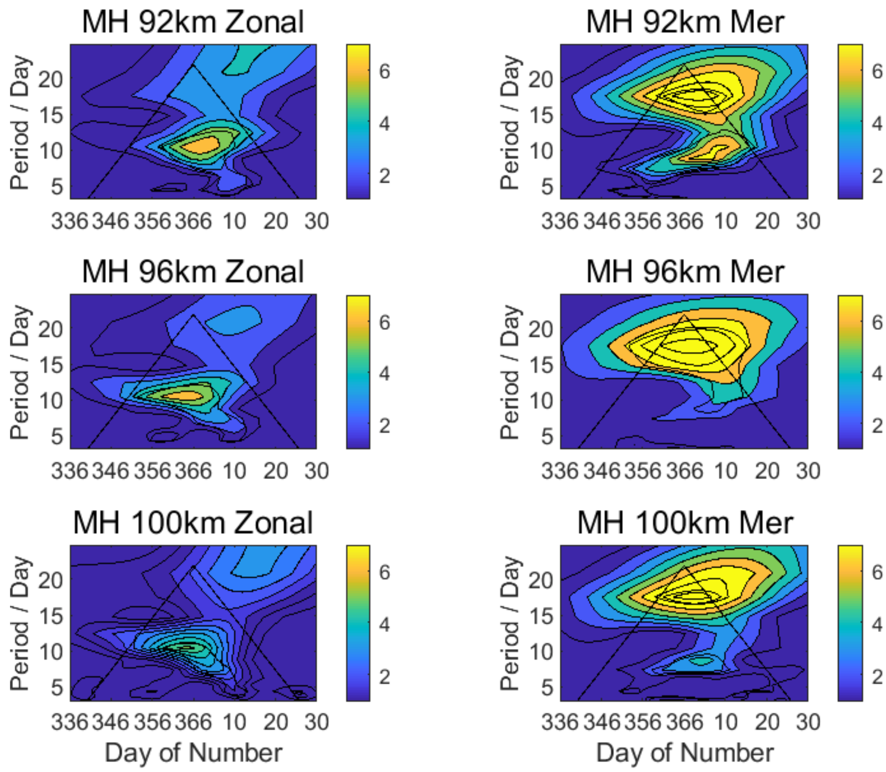

Figure5 Wavelet power spectra of zonal wind(left) and meridional wind(right) from December 1, 2012 to January 31, 2013 at Mohe station

.

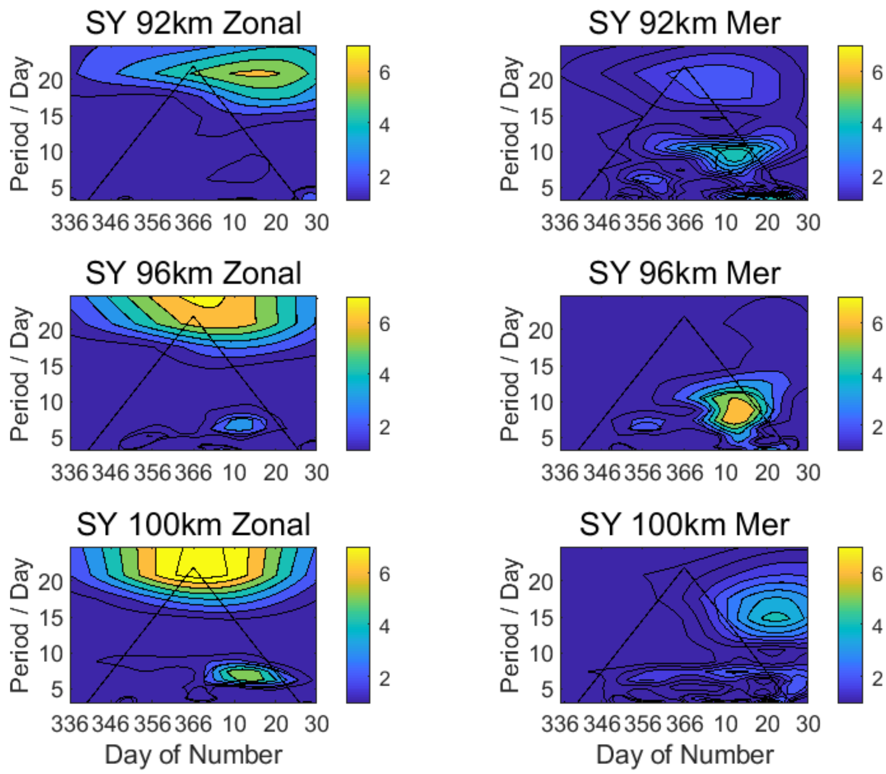

Figure6 Wavelet power spectra of zonal wind(left) and meridional wind(right)

from December 1, 2012 to January 31, 2013 at Sanya station

Discussion

Latitudinal and Longitudinal Dependence

Previous reports and our results have shown that there are significant ionospheric perturbations along latitudes and longitudes during SSW events. In terms of the 2013 SSW, Figure 3-4 show the TEC response on the chain 100°E, 110°E and 120°E ranging from 19.03°N to 49.21°N at latitude. The semi-diurnal perturbation in TEC that morning enhancement and afternoon depletion were observed along the chain 100°E and 110°E. It takes the equatorial ionization anomaly crest as dividing line and decreases toward the two poles gradually, indicating that there exists a latitudinal dependence in ionospheric response to 2013 SSW. Liu (2013) showed the semi-diurnal variations in MLT region is prominent at low and middle latitudes but not at high latitudes, and the latitudinal variations is predicted in model simulations to provide thermospheric background is important to ionosphere. Meanwhile, the latitudinal dependence may be related to the the ionosphere characteristic that electron density is the largest in the equatorial ionization anomaly crest at geomagnetic latitude˜±15°due to the equatorial fountain effect, and decreases toward the two poles gradually(Geetashree, 2020; Sumedha, 2021).

Figure 3 shows evident longitudinal dependence in ionosphere that the maximum deviation in TEC is 222% on the chain 120°E, which is more than 100°E and 110°E, but the afternoon depletion is weak. Geetashree (2020) studied the ionospheric response during 2013 SSW by TEC on the chain 10°E and 95°E, and discussed that the longitudinal differences might be attributed to the differential impact of the non-migrating tides and differences in the geomagnetic field elements between the two sectors. S. M. Liu (2019) studied that the semi-diurnal lunar tidal influence on low-latitudinal TEC tends to be more prominent in the American sector than in the East Asian sector during SSW events 2009-2018 and supported these differences due to the combined effect of tidal propagation and electrodynamic processes at these two sectors. In present work, the longitude difference is small between three chains, the geomagnetic field configuration is similar on different chains. Hence, the longitudinal ionospheric response in East Asia region during 2013 SSW may be attributed to differences in tidal influence on TEC by changing the [O/N2] ratio (Klimenko, 2013; Yasyukevich; 2018; Goncharenko, 2019).

Tide-PWs modulation

According to the above results and analysis, it is assumed that the ionosphere and lower atmosphere are probably coupled by the PWs forcing. The semi-diurnal tidal components of DTEC are extracted by harmonic fitting, with 2-day window and 1-day step, to analyze the coupling process between the semi-diurnal tidal components of TEC and PWs. Figure 7 shows the wavelet transform of semi-diurnal tidal components of DTEC at eighteen GPS stations. It indicates that the amplitudes of semi-diurnal tide at the latitude more than 23.87°N show obvious quasi 16-day wave-like oscillations along the chain 100°E and 110°E, while the quasi 10-day wave-like oscillations is weak relatively. But the quasi 10-day wave-like oscillations are clearly observed at YNMC, YNMH, GDZJ and QION stations located at low latitude. On the chain 120°E, the quasi 16-day wave-like oscillations are evident from LNYK (latitude: 40.69°N) to ZJWZ (latitude: 27.93°N), and they increase with the decrease of latitude. The results are consistent with the PWs fluctuations in the Mohe and Sanya in Figure5-6. According to the theory of PW-tidal modulation, the quasi 16-day PWs probably drive the TEC response by modulating tides at mid-latitude, and it might be attributed to the quasi-10 day planetary wave at low latitude.

The meridional and zonal winds are modulated by tides to change the electric field generated in layer E, which is mapped to layer F by magnetic field lines. This can drive the vertical drift of plasma and cause the ionospheric disturbance in the middle and low latitude (Liu, 2010). The ionospheric response, tide and planetary wave fluctuations in MLT region during the 2013 SSW further provide the coupling process of the ionosphere and MLT by tide-PWs modulation at middle and low latitudes.

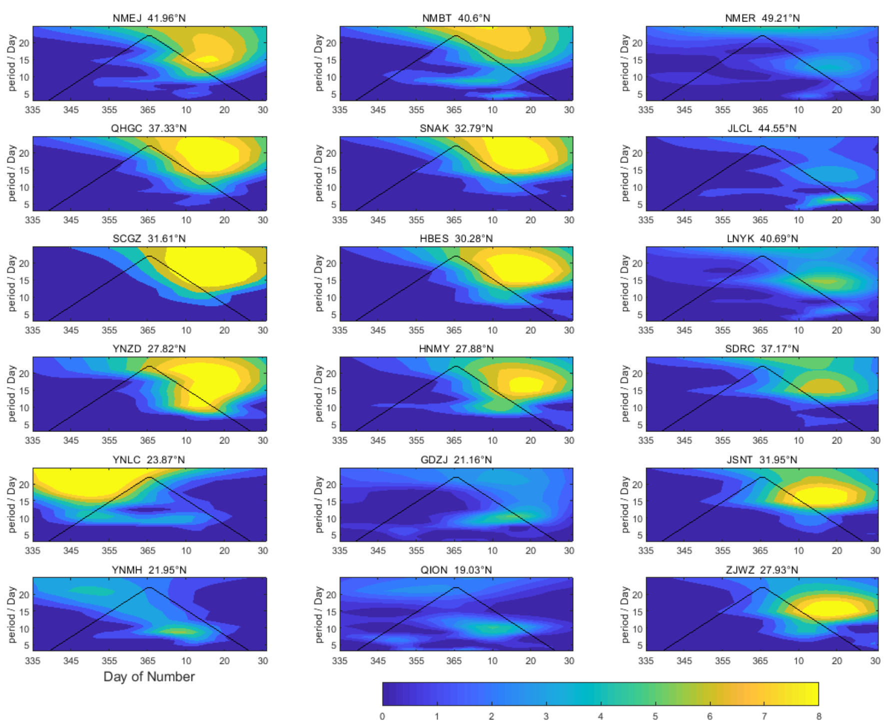

Figure7 Wavelet power spectra of DTEC semi-diurnal tidal component from December 1, 2012 to January 31, 2013 at all GPS TEC stations

conclusion

We use (a) TEC of three meridional chains with eighteen GPS stations at 100°E,110degE and 120degE, ranging from 19.03degN to 49.21degN, and (b) zonal wind and meridional winds of the Mohe and Sanya Meteor Radars to observe the ionospheric response to the 2013 SSW at middle and low latitudes. Apart from some result generally consistent with the work of Chen(2019) and Geetashree(2020), there are some new results. Our main conclusions are summarized as follows:

1) The TEC variations are mainly manifested by the semi-diurnal variations of morning enhancement and afternoon depletion during 2013 SSW, which is consistent with the results of many scholars (Liu, 2019; Geetashree, 2020). Meanwhile, the TEC variations exhibited latitudinal and longitudinal dependence. This may be due to semi-diurnal tides variations in MLT region and ionospheric characteristic.

2) We use zonal wind and meridional winds of Mohe meteor radar and Sanya meteor radar to analyze PWs fluctuations in MLT region at middle and low latitudes. The quasi 16-day planetary waves in meridional wind at Mohe are amplified at an altitude of 92-100 km . The quasi 10-day planetary waves at Sanya are amplified at an altitude of 96-100 km. This indicates that the winds may be the main driver of the ionospheric anomalies during 2013 SSW.

3) The12h tidal components in TEC are amplified in the middle and low latitudes ionosphere during the 2013 SSW. The amplitudes of the 12 h components in TEC exhibit a period of 16 days at middle latitude and 10 days at low latitude. This suggests that the semi-diurnal tides are modulated by the 16 day planetary waves at middle latitude and by the 10 day planetary waves at low latitude, further providing the PW-tide interaction theory at middle and low latitudes over the East Asia region.

Acknowledgments

This work was supported by the National Key R&D Program of China (No.2020YFB0505603), the National Natural Science Foundation of China Program (No.41674081) and the Stable-Support Scientific Project of China Research Institute of Radiowave Propagation(No.A132011W16). We acknowledge the use of TEC data from Crustal Movement Observation Network of China(CMONC). The zonal wind and meridional wind of meteor radars are obtained from the World Data System (WDS)(*http://wdc.geophys.cn/*). The stratospheric parameters are downloaded from the National Centers for Environmental Prediction (NCEP) (http://www.cpc.ncep.noaa.gov) and Goddard Space Flight Center(GSFC)(*https://avdc.gsfc.nasa.gov/*). The Kp and F10.7 index data are obtained from the GSFC/SPDF OMNI Web interface (*http://omniweb.gsfc.nasa.gov*).

References

Boris G Shpynev.(2015), High-midlatitude ionosphere response to major stratospheric warming. Earth, Planets and Space (2015) 67:18 DOI 10.1186/s40623-015-0187-1.

Chen, G., C. Wu, S. Zhang, B. Ning, X. Huang, D. Zhong, H. Qi, J. Wang, and L. Huang (2016), Midlatitude ionospheric responses to the 2013 SSW under high solar activity, J. Geophys. Res. Space Physics, 121, 790–803, doi:10.1002/ 2015JA021980.

Dora Panchevan, Plamen Mukhtarov. Stratospheric warmings: The atmosphere–ionosphere coupling paradigm. Journal of Atmospheric and Solar-Terrestrial Physics 73 (2011) 1697–1702.

Laskar, F.I., and D. Pallamraju (2014), Does sudden stratospheric warming induce meridional circulation in the mesosphere thermosphere system?, J.Geophys.Res. Space Physics, 119, 10,133-10,143,doi:10.1002/2014JA020086.

Liu, H.-L., and A. D. Richmond (2013), Attribution of ionospheric vertical plasma drift perturbations to large-scale waves and the dependence on solar activity, J. Geophys. Res. Space Physics, 118, 2452–2465, doi:10.1002/jgra.50265.

Lin, J. T., Lin, C. H., Lin, C. Y., Pedatella, N. M., Rajesh, P. K., Matsuo, T., & Liu, J. Y. (2019). Revisiting the modulations of ionospheric solar and lunar migrating tides during the 2009 stratospheric sudden warming by using global ionosphere pecifification. Space Weather, 17, 767–777. https://doi.org/10.1029/2019SW002184

Li,N. Luan, X., Lei, J., O. S.Bloaji, Owolabi, C., Chen, J., Xu, Z., Li. G, Ning, B(2020). variationss of mesospheric neutral winds and tides observed by a meteor radar chain over China during 2013 sudden stratospheric warming. JOURNAL OF GEOPHYSICAL RESEARCH: SPACE PHYSICS. https://doi.org/10.1029/2019JA027443.

LIU Kun, S H E N G Dongsheng, W A N G Feifei, Z H A N G Hongbo, LI Jianru. High precision algorithm for ionospheric V T E C based on single ground-based G N S S station (in Chinese). Chin. J. Space Sci., 2021, 41(3): 417-424. DOI: 10.11728/cjss2021.03.417

Luo, J., Gong, Y., Ma, Z., Zhang, S., Zhou, Q., Huang, C., et al. (2021). Study of the quasi 10-day waves in the MLT region during the 2018 February SSW by a meteor radar chain. Journal of Geophysical Research: Space Physics, 126, e2020JA028367. https://doi. org/10.1029/2020JA028367

J.R. Holton, H.-C. Tan, The inflfluence of the equatorial quasi-biennial oscillation on the global circulation at 50 mb. J. Atmos. Sci. 37, 2200–2208 (1980)

Geetashree Kakoti.,Bitap Raj Kalita et al(2020).Longitudinal and Interhemispheric ionospheric response to 2009 and 2013 SSW events in the African-European and Indian-East Asian sectors. American Geophysical Union. doi: 10.1029/2020JA028570

Guoqi Liu, Wengeng Huang.(2019). Ionospheric response to the 2018 sudden stratospheric warming event at mid- and low- latitude stations over China sector. American Geophysical Union doi: 10.1029/2019SW002160.

Jorge L. Chau, Larisa P. Goncharenko.(2012). Equatorial and Low Latitude Ionospheric Effects During Sudden Stratospheric Warming Events. Space Sci Rev (2012) 168:385–417. DOI 10.1007/s11214-011-9797-5.

Jonah, O. F., E. R. de Paula, E. A. Kherani, S. L. G. Dutra, and R. R. Paes(2014), Atmospheric and ionospheric response to sudden stratospheric warming of January 2013, J. Geophys. Res. Space Physics, 119,4973-4980,doi:10.1002/2013JA019491.

Fazlul I. Laskar.(2013) Investigations on vertical coupling of atmospheric regions using combined multiwavelength optical dayglow, magnetic, and radio measurements. JOURNAL OF GEOPHYSICAL RESEARCH: SPACE PHYSICS, VOL. 118, 4618–4627, doi:10.1002.

Fang, T.-W., T. Fuller-Rowell, H.Wang, R. Akmaev, and F.Wu(2014), Ionospheric response to sudden stratospheric warming events at low and high solar activity, J. Geophys. Res. Space Physics, 119,7858-7869, doi:10.1002/2014JA020142.

Korenkova, N.A., et al. Coupling between parameters of Es layer and planetary waves during SSW 2008, 2010. Adv. Space Res. (2015), http://dx.doi.org/10.1016/j.asr.2015.07.031.

Pancheva, D., and P. Mukhtarov (2011), Stratospheric warmings: The atmosphere-ionosphere coupling paradigm, J. Atmos. Sol. Terr. Phys., 73, 1697–1702, doi:10.1016/j.jastp.2011.03.006.

Sridharan, S. (2017), Solar and lunar tidal varibilities in GPS-TEC and geomagnetic field variationss: Seasonal as well as during the sudden stratospheric warming of 2010, J. Geophys. Res. Space Physics,122,4571-4587,doi:10.1002/2016JA023196.

Sumedha Gupta.(2021), Ionospheric Response to Sudden Stratospheric Warming Events Across Longitudes During Solar Cycle 24. Journal of Geophysical Research: Space Physics / Volume 126, Issue 10 / e2021JA029206

Sripathi, S., and A. Bhattacharyya (2012), Quiet time variability of the GPS TEC and EEJ strength over Indian region associated with major sudden stratospheric warming events during 2005/2006, J. Geophys.

Res., 117, A05305, https://doi.org/10.1029/2011JA017103.

Maute, A., M. E. Hagan, V. Yudin, H. L. Liu, and E. Yizengaw(2015), Causes of the longitudinal differences in the equatorial vertical ExB drift during the 2013 SSW period as simulated by the TIME-GCM, J.Geophys. Res. Space Physics, 120,5117-5136, doi:10.1002/2015JA021126.

Matthias, V., Hoffmann, P., Manson, A., Meek, C., Stober, G., Brown, P., & Rapp, M. (2013). The impact of planetary waves on the latitudinal displacement of sudden stratospheric warmings. Annales Geophysicae, 31(8), 1397–1415. https://doi.org/10.5194/angeo-31-1397-2013

N.M. Pedatella, J.M. Forbes, Evidence for stratosphere sudden warming-ionosphere coupling due to vertically propagating tides. Geophys. Res. Lett. 37(11), 1–5 (2010a). doi:10.1029/2010GL043560

Pedatella, N. M., A. D. Richmond, A.Maute, and H.-L. Liu(2016).Impact of semi-diurnal tidal variability during SSWs on the mean state of the ionosphere and thermosphere, J. Geophys. Res. Space Physics, 121, 8077-8088, doi:10.1002/2016JA022910.

T. Matsuno, A dynamical model of the stratospheric sudden warming. J. Atmos. Sci. 28, 1479–1494 (1971)

Upadhayaya, A. K., and K. K. Mahajan (2013), Ionospheric F2 region: Variability and sudden stratospheric warmings, J. Geophys. Res. Space Physics, 118, 6736–6750, doi:10.1002/jgra.50570.

Wang F F, Chen J S,Xu T, et a1. 2015. Response of the sporadic-E layer to the stratospheric sudden warming in January 2009.Chinese J.Geophys. (in Chinese). 58(3): 721-728, doi: 10. 6038 / cjg20150302.

Yasunobu Miyoshi and Yosuke Yamazaki. Excitation mechanism of ionospheric 6-day oscillation during the 2019 September sudden stratospheric warming event. American Geophysical Union. doi:10.1029/2020JA028283.

Yamazaki, Y., & Matthias, V. (2019). Large-amplitude quasi-10 day waves in the middle atmosphere during final warmings. Journal of Geophysical Research: Atmospheres, 124, 9874–9892. https://doi.org/10.1029/2019JD030634

Yu, F. R., Huang, K. M., Zhang, S. D., Huang, C. M., Yi, F., Gong, Y., et al. (2019). Quasi 10- and 16-day wave activities observed through meteor radar and MST radar during stratospheric fifinal warming in 2015 spring. Journal of Geophysical Research: Atmospheres, 124, 6040–6056. https://doi.org/10.1029/2019JD030630

The Ionospheric response During 2013 Stratospheric Sudden Warming over East Asia Region

Feifei Wang[1,2], Ji Tang[1], Xinjian Shan[1], Na Li[2], Hongbo Zhang[2],Dongsheng Sheng[2], Shuji Sun[2], Tong Xu[2]

1. *Institute of Geology China Earthquake Administration*
2. *Information center China Research Institute of Radiowave Propagation Qingdao, China*

Abstract

Ionospheric response to sudden stratospheric warming (SSW) are not well understood. During the 2013 SSW, ionospheric disturbances were observed in eighteen stations on three meridional chains of 100°E, 110°E and 120°E ranging from 19.03°N to 49.21°N at latitudes over East Asia region. The TEC response showed evident semi-diurnal disturbance that enhancement in the morning and depletion in the afternoon. The maximum TEC increased by more than 220% on the chain 120°E. In addition, the semi-diurnal disturbance of TEC were enhanced and indicated evident latitudinal and longitudinal dependence. The wavelet spectra of semi-diurnal disturbance in TEC presented quasi-16 day planetary wave-like oscillations at middle latitudes and quasi-10 day planetary wave-like oscillations at low latitudes. Meanwhile, the zonal winds and meridional winds at altitudes of 92-100 km showed quasi-16 day planetary wave at Mohe located middle latitude and quasi-10 day planetary wave at Sanya located low latitude, which are agree with semi-diurnal disturbance of TEC. Especially, the 12-hour component of TEC showed a quasi-16 day periodic component at middle latitude and a quasi-10 day periodic component at low latitude, indicating that the modulated semi-diurnal tides may transmit these 10 day and 16 day planetary wave-like oscillations to the ionosphere. The coupling between the atmosphere and ionosphere may be strengthened by the quasi-16 day waves at middle latitude and quasi-10 day waves at low latitude. This can further confirm the PW-tide interaction theory during the 2013 SSW and it is of significance in the middle and low latitude ionospheric response to SSW.

Key words: Ionosphere, SSW, MLT

1. Introduction

Stratospheric Sudden Warming (SSW) events are large-scale meteorological phenomena that usually occur in the Northern Hemisphere from December to February. SSWs are characterized by a rapid increase in the polar stratospheric temperature by several tens of degrees with a weakening or reversal of eastward zonal mean zonal winds. They result from the breaking of upward propagating stationary planetary waves (SPWs) from the troposphere to the stratosphere. These amplified SPWs interact with the stratospheric zonal mean flow and deposit their momentum in westward direction, resulting in an induced mean meridional circulation, which leads to a downwelling in the polar region and increases the temperature due to adiabatic heating (Matsuno, 1971; Hohon, 1980).

The ionized layer of the terrestrial atmosphere from ~90 to 1000 km above sea level called ionosphere which is mainly influenced by solar and geomagnetic activity. Apart from them, it has been more or less established during the last two decades that lower atmospheric wave processes also perturb the ionosphere significantly, accounting for ~20% of ionospheric variationss on average (Forbes, 2010), such as planetary wave, tide, gravity wave and so on. During the SSW, the tide may be modulated due to the planetary wave development, temperature and wind, which plays an important role in ionospheric response, and also provides a possible way to study the coupling between the Mesosphere and Lower Thermosphere(MLT) and ionosphere. As a result of SSWs, the ionospheric response is shown in Es layer and F layer in general. The response of Es layer during SSW is mainly focus on Es critical frequency (foEs) due to the PW and tide (Wang, 2015; Korenkova, 2015).

The ionospheric F region is shown to vary in terms of an anomalous daytime semi-diurnal signature in vertical plasma drift Maute,2015; Goncharenko, 2013), total electron content (TEC)(Liu, 2019; Geetashree, 2020), perturbations in electric fields(Sripathi, 2012), electron and neutral densities, electron and ion temperature, F layer parameters Chen, 2016 Pancheva, 2011 and the equatorial ionization anomaly (EIA) crest (Upadhayaya, 2013; Qiong, 2020). In addition, previous studies have showed the ionospheric response with latitude or longitude. Geetashree(2020) showed the latitudinal and longitudinal dependence in ionosphere during 2009 and 2013 SSW along the two meridional chains of 10°E and 95°E. Though the coupling mechanism of MLT region and ionospheric response during SSW is not clear, many researchers tried to explained by the neutral wind field electric field, PW, tide, even gravity waves(GW)(Laskar, 2014; Jonah, 2014).

Jonah(2014) studied the ionospheric response to the 2013 SSW in Brazilian sector using GPS TEC, geomagnetic data and Meteor Radar data. They found that the amplification of the 13-16 day period in TEC during the SSW and simultaneous amplification in zonal and meridional wind components in MLT region. Sripath(2012) analyzed the ionospheric TEC and EEJ effects during 2006 SSW, and found the quasi 16-day planetary waves modulate the tide. Chen(2019) studied the coupling process ionosphere and lower atmosphere during 2013 SSW using the foF2, hmF2 and Wuhan meteor radar data, and explained the ionospheric response through the theory of quasi 16-day planetary waves modulating tide at middle latitude.

However, only a few studies reported the association of the quasi-10-day PWs with SSW events. Matthias(2012) found that the quasi 10-day PWs and quasi 16-days waves were enhanced before and after the polar vortex breakdown with a composite analysis during SSW events in 2004, 2006, 2009, and 2010. Yamazaki (2019) reported slight enhancements of quasi-10-day PWs during some SSW events using the geopotential height data from 2004 to 2018. Luo(2021) showed that the quasi 10-day wave were increased during 2018 SSW at middle latitude.

In this study, we present the latitudinal and longitudinal dependence of the TEC response in East Asia region and the variations of wind in MLT region at middle and low latitudes during the 2013 SSW to further confirm the coupling mechanism by the theory of PW-tide modulation. In section 2 we introduce the data used in this paper, such as GPS TEC, wind, MLS temperature. In section 3 we present the variationss and 12-hour component of TEC and PWs in MLT before they are analyzed and discussed in section 4. Final conclusion are given in section 5.

1. Data

   (a) GPS TEC data

To study the ionospheric response to the major SSW, we used ground-based Global Positioning System (GPS)-derived vertical total electron content (TEC) for selected eighteen stations of Crustal Movement Observation Network of China(CMONC). These stations distribute along the meridional chains of 100°E 110°E and 120°E. Each chain consists of six stations covering varied latitudes from ~19.03°N to ~49.21°N. Table 1 shows the list of GPS stations. The KrigingKalman filter was used to resolve hardware delay and calculate vertical TEC (1TECU=1016) at 30-second intervals(LIU, 2021). We averaged the TEC 30-second intervals to 1-hour in units of TECu (1TECu = 10^{16} electrons/m) in the following.

- Table1 List of GPS stations

Sitename	**Longitude/°E**	**latitude/°N**	**Sitename**	**Longitude/°E**	**latitude/°N**
NMEJ	101.06	41.96	nmer	119.77	49.21
QHGC	100.14	37.33	jlcl	123.52	44.55
scgz	100.02	31.61	lnyk	122.61	40.69
ynzd	99.70	27.82	sdrc	122.42	37.17
ynlc	100.08	23.87	jsnt	120.89	31.95
ynmh	100.45	21.95	zjwz	120.76	27.93
nmbt	110.02	40.60	hnmy	109.8	27.88
snak	108.77	32.79	gdzj	110.31	21.16
hbes	109.49	30.28	qion	109.85	19.03

- 1. Meteor radar data

The zonal and meridional winds of meteor radar are from the World Data System (WDS) (http://wdc.geophys.cn/) to show the variations of planetary waves(PWs) in MLT region. We chose Mohe(122.3°E, 53.5°N) and Sanya(109.6°E, 18.3°N) meteor radars located middle and low latitudes, respectively. The average wind velocities were calculated from the meteor detection results by a least square fitting procedure embedded in the meteor radar software. The height coverage is from 70km to 110km, with the temporal and spatial resolutions are 1hour and 2km, respectively. Figure1 shows the map of GPS stations and Meteor radars used in this paper. GPS receiver stations are green circles, and Meteor radars are red diamonds.

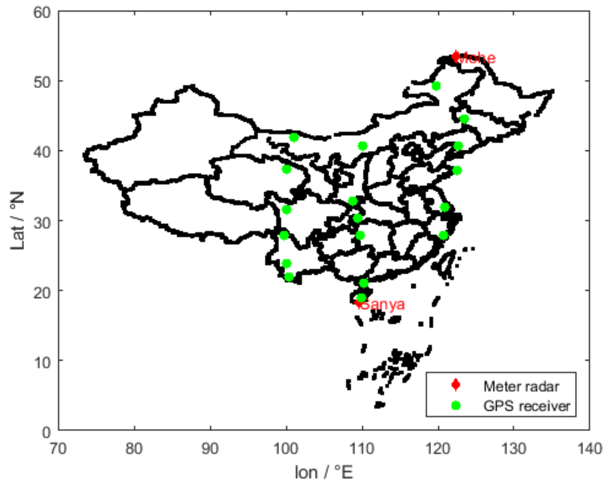

Figure1. The map of GPS receivers and Meteor radars.The green circles represent GPS receiver stations, and red diamonds represent the Meteor radars.

1. NCEP/NCAR Reanalysis data and Aura MLS data

The National Centers for Environmental Prediction(NCEP) and National Center for Atmospheric Research(NCAR) have cooperated in a project called reanalysis data that the temperature and wind are recovered from land surface, ship, rawinsonde, pilot balloon, aircraft, satellite, and other data (https://www.psl.noaa.gov//data/gridded/data.ncep.reanalysis.html). Daily averaged data are 2.5° $\times$ 2.5° grid for the whole world in latitude-longitude, 17 pressure levels from the Earth's surface up to 10 hPa. In this study, the stratospheric temperature at 10 hPa (approximately 30 km) at 60° N were used to obtain the temperature anomaly during 2013 SSW.

The Aura satellite was launched in July 2004. The angle between orbital plane and earth's equatorial plane is 82°, it rounds the earth 15 times a day. MLS(Microwave Limb Sounder, MLS) records atmospheric temperatures, density at different isobaric surfaces, 55 isobaric surfaces totally, corresponding height is 12~94km approximately (https://avdc.gsfc.nasa.gov/pub/data/satellite/Aura/MLS/V04/L2GP/Temperature/). In this paper, we used the MLS temperature data from December 1, 2012 to February 28, 2013 in the Northern Hemisphere to obtain the variations in temperature.

1. Results

   (a) 2012-2013 SSW

Figure2a-d show the temperatures, wind, Kp and F10.7 from December 1, 2012 to February 28, 2013. The stratospheric warming began on the first day of 2013 (January 1, 2013) from ~60km and gradually downward to ~45km, it reached a secondary peak on the fourth day(January 4, 2013), the temperature peak occurred on the twelfth day(January 12, 2013) and the zonal wind shifted from west to east, then the temperature recovered slowly. The solar and geomagnetic conditions are indicated by F10.7 and Kp indices, respectively, both available at the website http://omniweb.gsfc.nasa.gov/form/dx1.html. The F10.7 index is in Solar Flux Unit

(SFU = 10-22W/m2 /Hz). In this study, Kp 4 is considered geomagnetically quiet. During the 2013 SSW period, geomagnetic activity was quiet, kp index was not more than 4. F10.7 began to increase from January 2013, reaching the peak on January 10, F10.7=168. It's obvious that the solar activity was high during the 2013 SSW.

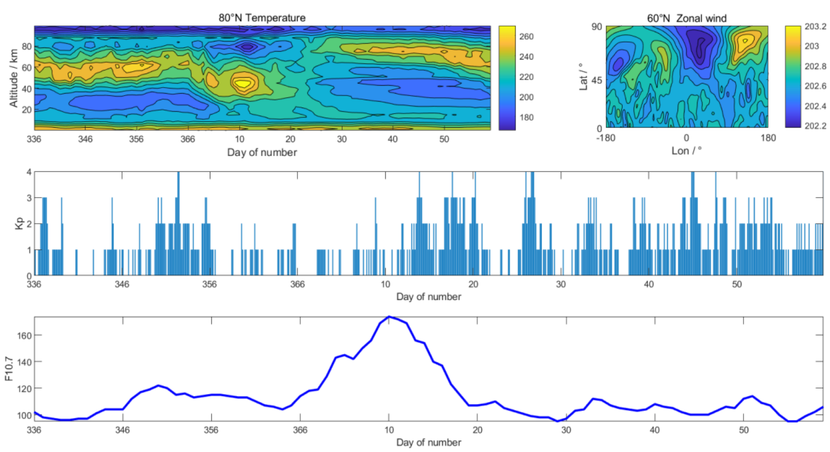

Figure2. The plots of temperatures, wind, F10.7 and Kp from December 1, 2012 to February 28, 2013. a) 80°N zonal averaged temperature. b) 60°N 10hpa zonal averaged wind on January 12. c) kp. d) F10.7.

1. Ionospheric response

To obtain the latitudinal and longitudinal differences in TEC during 2013 SSW , we chose eighteen GPS stations located along 100°E 110°E and 120°E covering 19.03°N to 49.21°N at latitude. The DTEC is the difference between the observed value(TEC) and the background value(TEC_{med}), which is used to extract the ionospheric disturbance. The background value TEC_{med} is the median value of TEC between December 1, 2012 and December 15, 2012.

Figure3 shows the variations of DTEC from January 1, 2013 to January 31, 2013, the two black dotted lines represent the peak time of the first temperature peak time (January 6) and the second peak time (January 12) , respectively.

We can see that the TEC enhancement at ~01:00-08:00(UT) and decrease at ~8:00-12:00(UT) everyday at all stations along the chain 100°E during January 4 to 17, 2013. In other words, enhancement in TEC during morning and early afternoon, and decrease in the afternoon. This TEC semi-diurnal disturbance becomes more and more obvious with decrease in latitude until the YNZD station (latitude: 27.82N), then the semi-diurnal disturbance weaken gradually at YNLC(latitude, 23.87°N) and YNMH(latitude, 21.95°N). The maximum and minimum deviation in TEC are 175% and -58% along the chain 100°E. The variations of TEC on the chain 110°E are similar to the chain 100°E. The TEC semi-diurnal disturbance increase with decrease in latitude until HNMY(latitude, 27.88°N). Meanwhile, GDZJ (latitude, 21.16°N) and QION(latitude, 19.03°N) located in low latitude both weaken. The maximum and minimum deviation in TEC are 150% and -53% of the chain 110°E. On the chain 120°E the variations of TEC are not clear at NMER latitude, 49.21°N and JLCL latitude, 44.55°N stations located at higher latitudes. The enhancement in TEC at morning is obvious from LNYK(latitude, 40.69°N) station and to the south until ZJWZ(latitude, 27.93°N) station, and the maximum deviation is 222%. But the decrease in TEC at afternoon is not clearly observed which is coincident with Chen(2019) along the chain 120°E .

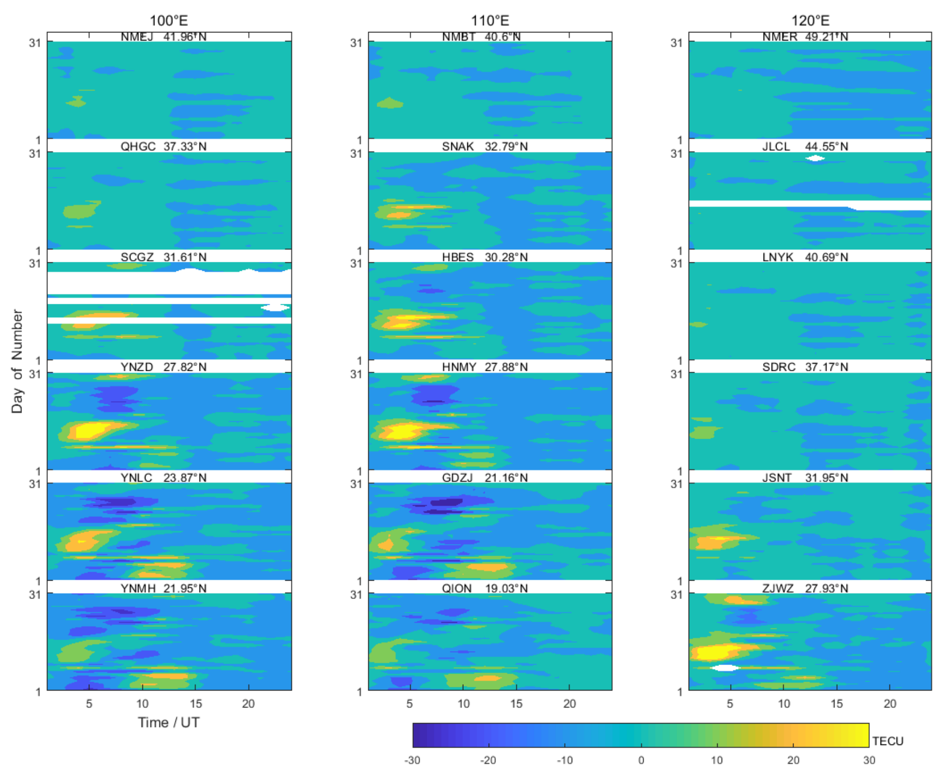

Figure3. variations of DTEC in TECu from January 1 to 31, 2013. The two black dotted lines represent the peak time of the first temperature peak (January 6) and the second peak time (January 12) , respectively.

From the above results, we can see that the TEC variations are not obvious when the latitude greater than 40°N. Inversely, the variations of TEC is obvious significantly with the decrease of latitude. The semi-diurnal variations of TEC in the form of morning enhancement and afternoon depletion are observed along the chain 100°E and 110°E and they increase with the decrease of latitude until ~27.82°N, then weaken significantly at YNLC, YNMH, GDZJ and QION stations located at latitudes less than 23.87°N. The TEC enhancement in the morning along the chain 120°E is evident, but weakening in the afternoon is not obvious. In a word, the TEC variations shows latitudinal dependence that the semi-diurnal variations in TEC takes equatorial ionization anomaly crest as the dividing line and weakens towards the two poles. Meanwhile, the longitudinal dependence in TEC variations is prominent during 2013 SSW. The TEC variations on the chain 100°E and 110°E are similar but different from the chain 120°E. The maximum deviation of TEC along the chain 120°E is larger than 100°E and 110°E, but the decrease at afternoon is not observed.

1. 12-hour component of TEC

The TEC semi-diurnal disturbance is evident with latitude in sector 3.2. Figure 4 shows the wavelet power spectra of DTEC between January 1 to 31, 2013 to further analyze DTEC periodic variations. It can be seen that the DTEC have prominent 12-hour component period and the latitudinal characteristic is coincident with DTEC variations shown in Figure3. Hence, both DTEC and 12-hour component of DTEC take the equatorial ionization anomaly crest as the dividing line, decrease toward the two poles gradually, and disappear at higher latitude finally. As we all know that the tides occur mainly in MLT region and have maximum amplitudes in this region, they can affect the middle and low latitude ionosphere by modulating E-layer generators. It is assumed that the TEC semi-diurnal disturbance is caused by the semi-diurnal tide enhancement at the middle and low latitudes during 2013 SSW.

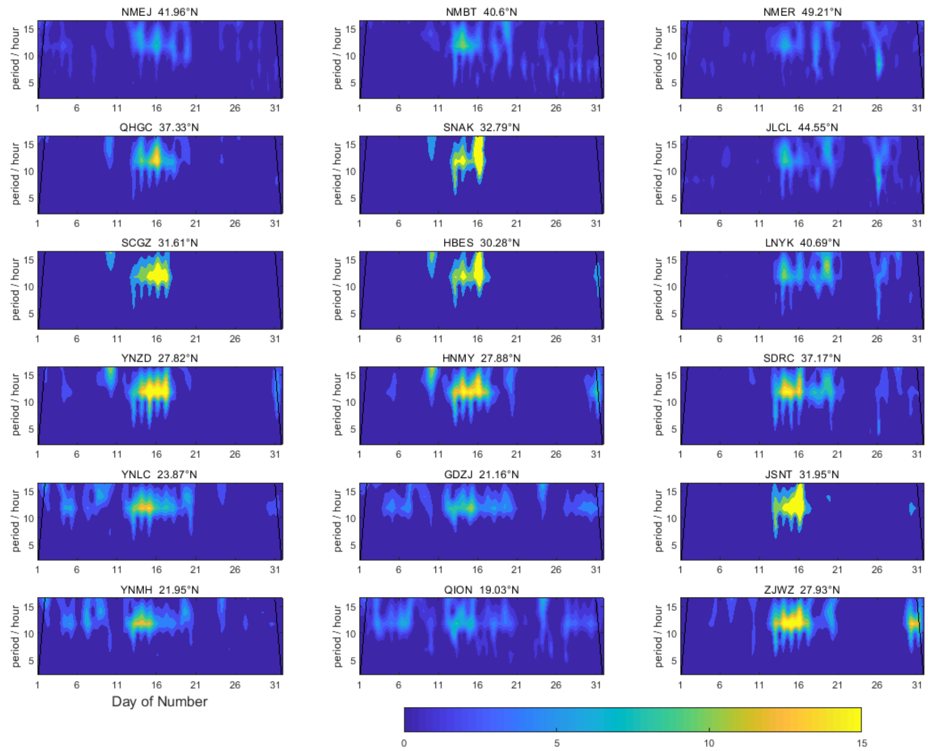

Figure4. Wavelet power spectra of DTEC between January 1 to 31, 2013.

1. Planetary wave variations in MLT

The zonal and meridional winds of Mohe and Sanya meteor radars were used to analyze the Planetary waves(PWs) variations in MLT region during the 2013 SSW at middle and low latitudes, respectively. The two radars can observe meridional and zonal winds at an altitude from 70km to 110km, with a altitude resolution of 2km and a time resolution of 1h. Considering the data quality, only the wind data at 92km, 96km and 100km heights were selected and processed the time resolution from 1h to 24h. Figure5-6 show the zonal and meridional winds wavelet power spectra at the 92km, 96km and 100km of Mohe and Sanya station, respectively. The quasi 10-Day planetary wave amplitudes are enhanced in zonal wind at Mohe all altitudes from December 20, 2012 to January 10, 2013 before warming, and the maximum amplitude is 7m/s at 92km. Quasi-16-day planetary wave amplitudes are enhanced in meridional wind from December 11, 2012 to January 27, 2013, and the maximum amplitude is 13.4m/s. Hence the quasi 16-day wave amplitude is higher than quasi 10-day wave amplitude at Mohe station. At Sanya, quasi-10-day planetary wave amplitudes are increased at all altitudes except for the 92km zonal wind, and the maximum amplitude is

7m/s. In general, the qusai-16-day waves are enhanced mainly at Mohe located at middle latitude and the qusai-10-day waves mainly at Sanya located at low latitude which are consistent with the variations of quasi-10-day and quasi-16-day planetary waves during SFW event in 2015 analyzed by Yu(2019).

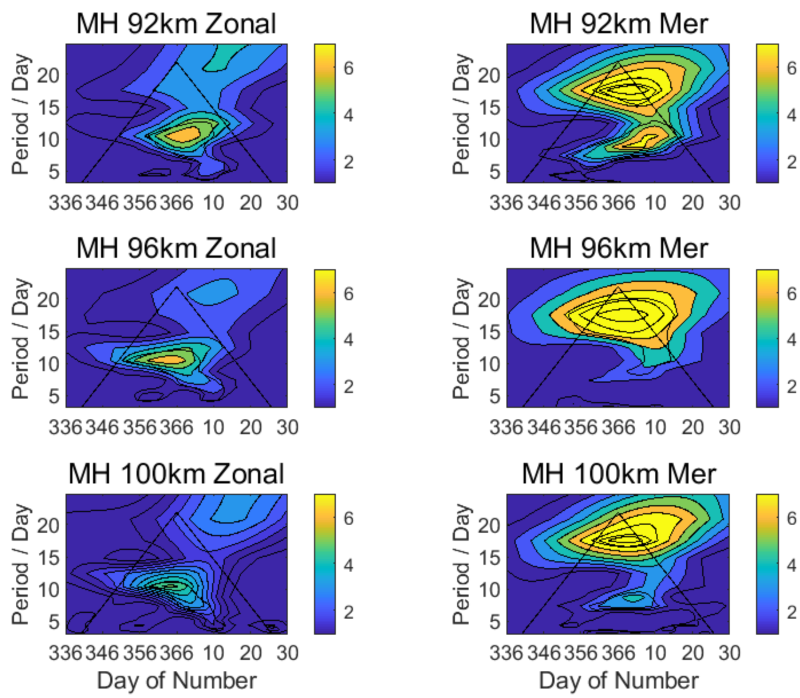

- Figure5 Wavelet power spectra of zonal wind(left) and meridional wind(right)
- from December 1, 2012 to January 31, 2013 at Mohe station

.

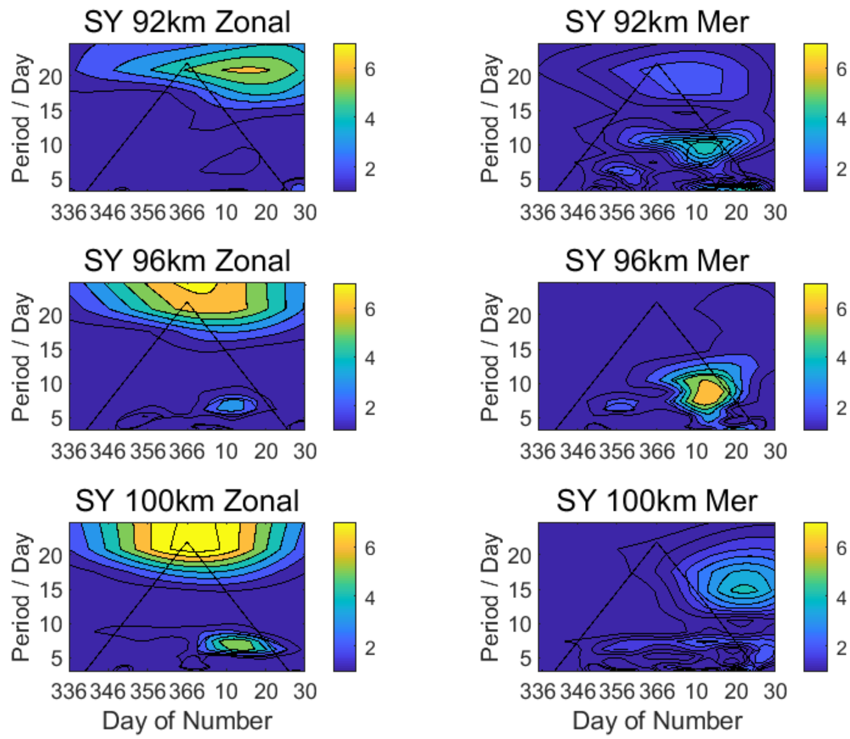

- Figure6 Wavelet power spectra of zonal wind(left) and meridional wind(right)
- from December 1, 2012 to January 31, 2013 at Sanya station

1. Discussion

    (a) Latitudinal and Longitudinal Dependence

Previous reports and our results have shown that there are significant ionospheric perturbations along latitudes and longitudes during SSW events. In terms of the 2013 SSW, Figure 3-4 show the TEC response on the chain 100°E, 110°E and 120°E ranging from 19.03°N to 49.21°N at latitude. The semi-diurnal perturbation in TEC that morning enhancement and afternoon depletion were observed along the chain 100°E and 110°E. It takes the equatorial ionization anomaly crest as dividing line and decreases toward the two poles gradually, indicating that there exists a latitudinal dependence in ionospheric response to 2013 SSW. Liu (2013) showed the semi-diurnal variations in MLT region is prominent at low and middle latitudes but not at high latitudes, and the latitudinal variations is predicted in model simulations to provide thermospheric background is important to ionosphere. Meanwhile, the latitudinal dependence may be related to the the ionosphere characteristic that electron density is the largest in the equatorial ionization anomaly crest at geomagnetic latitude~±15°due to the equatorial fountain effect, and decreases toward the two poles gradually(Geetashree, 2020; Sumedha, 2021).

Figure 3 shows evident longitudinal dependence in ionosphere that the maximum deviation in TEC is 222% on the chain 120°E, which is more than 100°E and 110°E, but the afternoon depletion is weak. Geetashree (2020) studied the ionospheric response during 2013 SSW by TEC on the chain 10°E and 95°E, and discussed that the longitudinal differences might be attributed to the differential impact of the non-migrating tides and differences in the geomagnetic field elements between the two sectors. S. M. Liu (2019) studied that the semi-diurnal lunar tidal influence on low-latitudinal TEC tends to be more prominent in the American sector than in the East Asian sector during SSW events 2009-2018 and supported these differences due to the combined effect of tidal propagation and electrodynamic processes at these two sectors. In present work, the longitude difference is small between three chains, the geomagnetic field configuration is similar on different chains. Hence, the longitudinal ionospheric response in East Asia region during 2013 SSW may be attributed to differences in tidal influence on TEC by changing the [O/N2] ratio (Klimenko, 2013; Yasyukevich; 2018; Goncharenko, 2019).

1. Tide-PWs modulation

According to the above results and analysis, it is assumed that the ionosphere and lower atmosphere are probably coupled by the PWs forcing. The semi-diurnal tidal components of DTEC are extracted by harmonic fitting, with 2-day window and 1-day step, to analyze the coupling process between the semi-diurnal tidal components of TEC and PWs. Figure 7 shows the wavelet transform of semi-diurnal tidal components of DTEC at eighteen GPS stations. It indicates that the amplitudes of semi-diurnal tide at the latitude more than 23.87°N show obvious quasi 16-day wave-like oscillations along the chain 100°E and 110°E, while the quasi 10-day wave-like oscillations is weak relatively. But the quasi 10-day wave-like oscillations are clearly observed at YNMC, YNMH, GDZJ and QION stations located at low latitude. On the chain 120°E, the quasi 16-day wave-like oscillations are evident from LNYK (latitude: 40.69°N) to ZJWZ (latitude: 27.93°N), and they increase with the decrease of latitude. The results are consistent with the PWs fluctuations in the Mohe and Sanya in Figure5-6. According to the theory of PW-tidal modulation, the quasi 16-day PWs probably drive the TEC response by modulating tides at mid-latitude, and it might be attributed to the quasi-10 day planetary wave at low latitude.

The meridional and zonal winds are modulated by tides to change the electric field generated in layer E, which is mapped to layer F by magnetic field lines. This can drive the vertical drift of plasma and cause the ionospheric disturbance in the middle and low latitude (Liu, 2010). The ionospheric response, tide and planetary wave fluctuations in MLT region during the 2013 SSW further provide the coupling process of the ionosphere and MLT by tide-PWs modulation at middle and low latitudes.

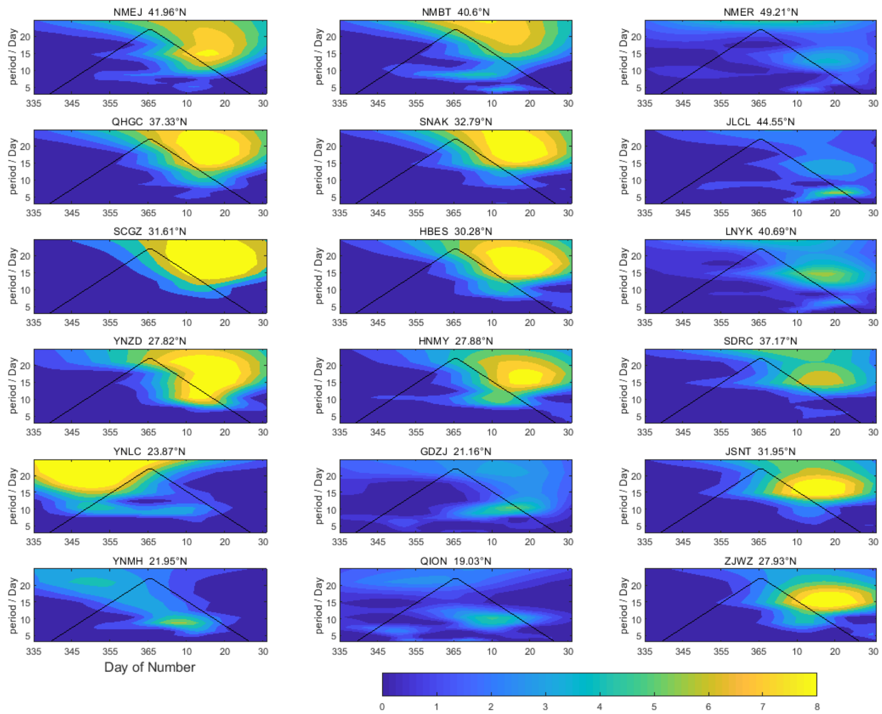

- Figure7 Wavelet power spectra of DTEC semi-diurnal tidal component from December 1, 2012 to January 31, 2013 at all GPS TEC stations

1. conclusion

We use (a) TEC of three meridional chains with eighteen GPS stations at 100°E 110°E and 120°E, ranging from 19.03°N to 49.21°N, and (b) zonal wind and meridional winds of the Mohe and Sanya Meteor Radars to observe the ionospheric response to the 2013 SSW at middle and low latitudes. Apart from some result generally consistent with the work of Chen(2019) and Geetashree(2020), there are some new results. Our main conclusions are summarized as follows:

1) The TEC variations are mainly manifested by the semi-diurnal variations of morning enhancement and afternoon depletion during 2013 SSW, which is consistent with the results of many scholars (Liu, 2019; Geetashree, 2020). Meanwhile, the TEC variations exhibited latitudinal and longitudinal dependence. This may be due to semi-diurnal tides variations in MLT region and ionospheric characteristic.

2) We use zonal wind and meridional winds of Mohe meteor radar and Sanya meteor radar to analyze PWs fluctuations in MLT region at middle and low latitudes. The quasi 16-day planetary waves in meridional wind at Mohe are amplified at an altitude of 92-100 km . The quasi 10-day planetary waves at

Sanya are amplified at an altitude of 96-100 km. This indicates that the winds may be the main driver of the ionospheric anomalies during 2013 SSW.

3) The12h tidal components in TEC are amplified in the middle and low latitudes ionosphere during the 2013 SSW. The amplitudes of the 12 h components in TEC exhibit a period of 16 days at middle latitude and 10 days at low latitude. This suggests that the semi-diurnal tides are modulated by the 16 day planetary waves at middle latitude and by the 10 day planetary waves at low latitude, further providing the PW-tide interaction theory at middle and low latitudes over the East Asia region.

Acknowledgments

This work was supported by the National Key R&D Program of China (No.2020YFB0505603), the National Natural Science Foundation of China Program (No.41674081) and the Stable-Support Scientific Project of China Research Institute of Radiowave Propagation(No.A132011W16). We acknowledge the use of TEC data from Crustal Movement Observation Network of China(CMONC). The zonal wind and meridional wind of meteor radars are obtained from the World Data System (WDS)(http://wdc.geophys.cn/). The stratospheric parameters are downloaded from the National Centers for Environmental Prediction (NCEP) (http://www.cpc.ncep.noaa.gov) and Goddard Space Flight Center(GSFC)(https://avdc.gsfc.nasa.gov/). The Kp and F10.7 index data are obtained from the GSFC/SPDF OMNI Web interface (http://omniweb.gsfc.nasa.gov).

•

References

Boris G Shpynev.(2015), High-midlatitude ionosphere response to major stratospheric warming. Earth, Planets and Space (2015) 67:18 DOI 10.1186/s40623-015-0187-1.

Chen, G., C. Wu, S. Zhang, B. Ning, X. Huang, D. Zhong, H. Qi, J. Wang, and L. Huang (2016), Midlatitude ionospheric responses to the 2013 SSW under high solar activity, J. Geophys. Res. Space Physics, 121, 790–803, doi:10.1002/2015JA021980.

Dora Panchevan, Plamen Mukhtarov. Stratospheric warmings: The atmosphere–ionosphere coupling paradigm. Journal of Atmospheric and Solar-Terrestrial Physics 73 (2011) 1697–1702.

Laskar, F.I., and D. Pallamraju (2014), Does sudden stratospheric warming induce meridional circulation in the mesosphere thermosphere system?, J.Geophys.Res. Space Physics, 119, 10,133-10,143,doi:10.1002/2014JA020086.

Liu, H.-L., and A. D. Richmond (2013), Attribution of ionospheric vertical plasma drift perturbations to large-scale waves and the dependence on solar activity, J. Geophys. Res. Space Physics, 118, 2452–2465, doi:10.1002/jgra.50265.

Lin, J. T., Lin, C. H., Lin, C. Y., Pedatella, N. M., Rajesh, P. K., Matsuo, T., & Liu, J. Y. (2019). Revisiting the modulations of ionospheric solar and lunar migrating tides during the 2009 stratospheric sudden warming by using global ionosphere pecififcation. Space Weather, 17, 767–777. https://doi.org/10.1029/2019SW002184

Li, . Luan, X., Lei, J., O. S. loaji, Owolabi, C., Chen, J., Xu, Z., Li. G, Ning, B(2020). variationss of mesospheric neutral winds and tides observed by a meteor radar chain over China during 2013 sudden stratospheric warming. JOURNAL OF GEOPHYSICAL RESEARCH: SPACE PHYSICS. https://doi.org/10.1029/2019JA027443.

LIU Kun, S H E N G Dongsheng, W A N G Feifei, Z H A N G Hongbo, LI Jianru. High precision algorithm for ionospheric V T E C based on single ground-based G N S S station (in Chinese). Chin. J. Space Sci., 2021, 41(3): 417-424. DOI: 10.11728/cjss2021.03.417

Luo, J., Gong, Y., Ma, Z., Zhang, S., Zhou, Q., Huang, C., et al. (2021). Study of the quasi 10-day waves in the MLT region during the 2018 February SSW by a meteor radar chain. Journal of Geophysical Research: Space Physics, 126, e2020JA028367. https://doi. org/10.1029/2020JA028367

J.R. Holton, H.-C. Tan, The inflfluence of the equatorial quasi-biennial oscillation on the global circulation at 50 mb. J. Atmos. Sci. 37, 2200–2208 (1980)

Geetashree Kakoti.,Bitap Raj Kalita et al(2020).Longitudinal and Interhemispheric ionospheric response to 2009 and 2013 SSW events in the African-European and Indian-East Asian sectors. American Geophysical Union. doi: 10.1029/2020JA028570

Guoqi Liu, Wengeng Huang.(2019). Ionospheric response to the 2018 sudden stratospheric warming event at mid- and low- latitude stations over China sector. American Geophysical Union doi: 10.1029/2019SW002160.

Jorge L. Chau, Larisa P. Goncharenko.(2012). Equatorial and Low Latitude Ionospheric Effects During Sudden Stratospheric Warming Events. Space Sci Rev (2012) 168:385–417. DOI 10.1007/s11214-011-9797-5.

Jonah, O. F., E. R. de Paula, E. A. Kherani, S. L. G. Dutra, and R. R. Paes(2014), Atmospheric and ionospheric response to sudden stratospheric warming of January 2013, J. Geophys. Res. Space Physics, 119,4973-4980,doi:10.1002/2013JA019491.

Fazlul I. Laskar.(2013) Investigations on vertical coupling of atmospheric regions using combined multiwavelength optical dayglow, magnetic, and radio measurements. JOURNAL OF GEOPHYSICAL RESEARCH: SPACE PHYSICS, VOL. 118, 4618–4627, doi:10.1002.

Fang, T.-W., T. Fuller-Rowell, H.Wang, R. Akmaev, and F.Wu(2014), Ionospheric response to sudden stratospheric warming events at low and high solar activity, J. Geophys. Res. Space Physics, 119,7858-7869, doi:10.1002/2014JA020142.

Korenkova, N.A., et al. Coupling between parameters of Es layer and planetary waves during SSW 2008, 2010. Adv. Space Res. (2015), http://dx.doi.org/10.1016/j.asr.2015.07.031.

Pancheva, D., and P. Mukhtarov (2011), Stratospheric warmings: The atmosphere-ionosphere coupling paradigm, J. Atmos. Sol. Terr. Phys., 73, 1697–1702, doi:10.1016/j.jastp.2011.03.006.

Sridharan, S. (2017), Solar and lunar tidal varibilities in GPS-TEC and geomagnetic field variationss: Seasonal as well as during the sudden stratospheric warming of 2010, J. Geophys. Res. Space Physics,122,4571-4587,doi:10.1002/2016JA023196.

Sumedha Gupta.(2021), Ionospheric Response to Sudden Stratospheric Warming Events Across Longitudes During Solar Cycle 24. Journal of Geophysical Research: Space Physics / Volume 126, Issue 10 / e2021JA029206

Sripathi, S., and A. Bhattacharyya (2012), Quiet time variability of the GPS TEC and EEJ strength over Indian region associated with major sudden stratospheric warming events during 2005/2006, J. Geophys. Res., 117, A05305, https://doi.org/10.1029/2011JA017103.

Maute, A., M. E. Hagan, V. Yudin, H. L. Liu, and E. Yizengaw(2015), Causes of the longitudinal differences in the equatorial vertical E×B drift during the 2013 SSW period as simulated by the TIME-GCM, J.Geophys. Res. Space Physics, 120,5117-5136, doi:10.1002/2015JA021126.

Matthias, V., Hoffmann, P., Manson, A., Meek, C., Stober, G., Brown, P., & Rapp, M. (2013). The impact of planetary waves on the latitudinal displacement of sudden stratospheric warmings. Annales Geophysicae, 31(8), 1397–1415. https://doi.org/10.5194/angeo-31-1397-2013

N.M. Pedatella, J.M. Forbes, Evidence for stratosphere sudden warming-ionosphere coupling due to vertically propagating tides. Geophys. Res. Lett. 37(11), 1–5 (2010a). doi:10.1029/2010GL043560

Pedatella, N. M., A. D. Richmond, A.Maute, and H.-L. Liu(2016).Impact of semi-diurnal tidal variability during SSWs on the mean state of the ionosphere and thermosphere, J. Geophys. Res. Space Physics, 121, 8077-8088, doi:10.1002/2016JA022910.

T. Matsuno, A dynamical model of the stratospheric sudden warming. J. Atmos. Sci. 28, 1479–1494 (1971)

Upadhayaya, A. K., and K. K. Mahajan (2013), Ionospheric F2 region: Variability and sudden stratospheric warmings, J. Geophys. Res. Space Physics, 118, 6736–6750, doi:10.1002/jgra.50570.

Wang F F, Chen J S Xu T, et a1. 2015. Response of the sporadic-E layer to the stratospheric sudden warming in January 2009 Chinese J Geophys. (in Chinese). 58(3): 721-728, doi: 10. 6038 / cjg20150302.

Yasunobu Miyoshi and Yosuke Yamazaki. Excitation mechanism of ionospheric 6-day oscillation during the 2019 September sudden stratospheric warming event. American Geophysical Union. doi:10.1029/2020JA028283.

Yamazaki, Y., & Matthias, V. (2019). Large-amplitude quasi-10 day waves in the middle atmosphere during final warmings. Journal of Geophysical Research: Atmospheres, 124, 9874–9892. https://doi.org/10.1029/2019JD030634

Yu, F. R., Huang, K. M., Zhang, S. D., Huang, C. M., Yi, F., Gong, Y., et al. (2019). Quasi 10- and 16-day wave activities observed through meteor radar and MST radar during stratospheric fifinal warming in 2015 spring. Journal of Geophysical Research: Atmospheres, 124, 6040–6056. https://doi.org/10.1029/2019JD030630

The Ionospheric response During 2013 Stratospheric Sudden Warming over East Asia Region

Feifei Wang[1,2], Ji Tang[1], Xinjian Shan[1], Na Li[2], Hongbo Zhang[2],Dongsheng Sheng[2], Shuji Sun[2], Tong Xu[2]

1. *Institute of Geology China Earthquake Administration*
2. *Information center China Research Institute of Radiowave Propagation Qingdao, China*

Abstract

Ionospheric response to sudden stratospheric warming (SSW) are not well understood. During the 2013 SSW, ionospheric disturbances were observed in eighteen stations on three meridional chains of 100°E, 110°E and 120°E ranging from 19.03°N to 49.21°N at latitudes over East Asia region. The TEC response showed evident semi-diurnal disturbance that enhancement in the morning and depletion in the afternoon. The maximum TEC increased by more than 220% on the chain 120° E. In addition, the semi-diurnal disturbance of TEC were enhanced and indicated evident latitudinal and longitudinal dependence. The wavelet spectra of semi-diurnal disturbance in TEC presented quasi-16 day planetary wave-like oscillations at middle latitudes and quasi-10 day planetary wave-like oscillations at low latitudes. Meanwhile, the zonal winds and meridional winds at altitudes of 92-100 km showed quasi-16 day planetary wave at Mohe located middle latitude and quasi-10 day planetary wave at Sanya located low latitude, which are agree with semi-diurnal disturbance of TEC. Especially, the 12-hour component of TEC showed a quasi-16 day periodic component at middle latitude and a quasi-10 day periodic component at low latitude, indicating that the modulated semi-diurnal tides may transmit these 10 day and 16 day planetary wave-like oscillations to the ionosphere. The coupling between the atmosphere and ionosphere may be strengthened by the quasi-16 day waves at middle latitude and quasi-10 day waves at low latitude. This can further confirm the PW-tide interaction theory during the 2013 SSW and it is of significance in the middle and low latitude ionospheric response to SSW.

Key words: Ionosphere, SSW, MLT

1. Introduction

Stratospheric Sudden Warming (SSW) events are large-scale meteorological phenomena that usually occur in the Northern Hemisphere from December to February. SSWs are characterized by a rapid increase in the polar stratospheric temperature by several tens of degrees with a weakening or reversal of eastward zonal mean zonal winds. They result from the breaking of upward propagating stationary planetary waves (SPWs) from the troposphere to the stratosphere. These amplified SPWs interact with the stratospheric zonal mean flow and deposit their momentum in westward direction, resulting in an induced mean meridional circulation, which leads to a downwelling in the polar region and increases the temperature due to adiabatic heating (Matsuno, 1971; Hohon, 1980).

The ionized layer of the terrestrial atmosphere from ~90 to 1000 km above sea level called ionosphere which is mainly influenced by solar and geomagnetic activity. Apart from them, it has been more or less established during the last two decades that lower atmospheric wave processes also perturb the ionosphere significantly, accounting for ~20% of ionospheric variationss on average (Forbes, 2010), such as planetary wave, tide, gravity wave and so on. During the SSW, the tide may be modulated due to the planetary wave development, temperature and wind, which plays an important role in ionospheric response, and also provides a possible way to study the coupling between the Mesosphere and Lower Thermosphere(MLT) and ionosphere. As a result of SSWs, the ionospheric response is shown in Es layer and F layer in general. The response of Es layer during SSW is mainly focus on Es critical frequency (foEs) due to the PW and tide (Wang, 2015; Korenkova, 2015).

The ionospheric F region is shown to vary in terms of an anomalous daytime semi-diurnal signature in vertical plasma drift（Maute,2015; Goncharenko, 2013), total electron content (TEC)(Liu, 2019; Geetashree, 2020), perturbations in electric fields(Sripathi, 2012), electron and neutral densities, electron and ion temperature, F layer parameters（Chen, 2016；Pancheva, 2011）and the equatorial ionization anomaly (EIA) crest (Upadhayaya, 2013; Qiong, 2020). In addition, previous studies have showed the ionospheric response with latitude or longitude. Geetashree(2020) showed the latitudinal and longitudinal dependence in ionosphere during 2009 and 2013 SSW along the two meridional chains of 10° E and 95° E. Though the coupling mechanism of MLT region and ionospheric response during SSW is not clear, many researchers tried to explained by the neutral wind field，electric field, PW, tide, even gravity waves(GW)(Laskar, 2014; Jonah, 2014).

Jonah(2014) studied the ionospheric response to the 2013 SSW in Brazilian sector using GPS TEC, geomagnetic data and Meteor Radar data. They found that the amplification of the 13-16 day period in TEC during the SSW and simultaneous amplification in zonal and meridional wind components in MLT region. Sripath(2012) analyzed the ionospheric TEC and EEJ effects during 2006 SSW, and found the quasi 16-day planetary waves modulate the tide. Chen(2019) studied the coupling process ionosphere and lower atmosphere during 2013 SSW using the foF2, hmF2 and Wuhan meteor radar data, and explained the ionospheric response through the theory of quasi 16-day planetary waves modulating tide at middle latitude.

However, only a few studies reported the association of the quasi-10-day PWs with SSW events. Matthias(2012) found that the quasi 10-day PWs and quasi 16-days waves were enhanced before and after the polar vortex breakdown with a composite analysis during SSW events in 2004, 2006, 2009, and 2010. Yamazaki (2019) reported slight enhancements of quasi-10-day PWs during some SSW events using the geopotential height data from 2004 to 2018. Luo(2021) showed that the quasi 10-day wave were increased during 2018 SSW at middle latitude.

In this study, we present the latitudinal and longitudinal dependence of the TEC response in East Asia region and the variations of wind in MLT region at middle and low latitudes during the 2013 SSW to further confirm the coupling mechanism by the theory of PW-tide modulation. In section 2 we introduce the data used in this paper, such as GPS TEC, wind, MLS temperature. In section 3 we present the variationss and 12-hour component of TEC and PWs in MLT before they are analyzed and discussed in section 4. Final conclusion are given in section 5.

2. Data

2.1 GPS TEC data

To study the ionospheric response to the major SSW, we used ground-based Global Positioning System (GPS)-derived vertical total electron content (TEC) for selected eighteen stations of Crustal Movement Observation Network of China(CMONC). These stations distribute along the meridional chains of 100° E、110° E and 120° E. Each chain consists of six stations covering varied latitudes from ~19.03° N to ~49.21° N. Table 1 shows the list of GPS stations. The KrigingKalman filter was used to resolve hardware delay and calculate vertical TEC (1TECU=1016) at 30-second intervals(LIU, 2021). We averaged the TEC 30-second intervals to 1-hour in units of TECu (1TECu = 10^{16} electrons/m) in the following.

Table1 List of GPS stations

Sitename	Longitude/° E	latitude/° N	Sitename	Longitude/° E	latitude/° N
NMEJ	101.06	41.96	NMER	119.77	49.21
QHGC	100.14	37.33	JLCL	123.52	44.55
SCGZ	100.02	31.61	LNYK	122.61	40.69
YNZD	99.70	27.82	SDRC	122.42	37.17
YNLC	100.08	23.87	JSNT	120.89	31.95
YNMH	100.45	21.95	ZJWZ	120.76	27.93
NMBT	110.02	40.60	HNMY	109.8	27.88
SNAK	108.77	32.79	GDZJ	110.31	21.16
HBES	109.49	30.28	QION	109.85	19.03

2.2 Meteor radar data

The zonal and meridional winds of meteor radar are from the World Data System (WDS) (http://wdc.geophys.cn/) to show the variations of planetary waves(PWs) in MLT region. We chose Mohe(122.3° E, 53.5° N) and Sanya(109.6° E, 18.3° N) meteor radars located middle and low latitudes, respectively. The average wind velocities were calculated from the meteor detection results by a least square fitting procedure embedded in the meteor radar software. The height coverage is from 70km to 110km, with the temporal and spatial resolutions are 1hour and 2km, respectively. Figure1 shows the map of GPS stations and Meteor radars used in this paper. GPS receiver stations are green circles, and Meteor radars are red diamonds.

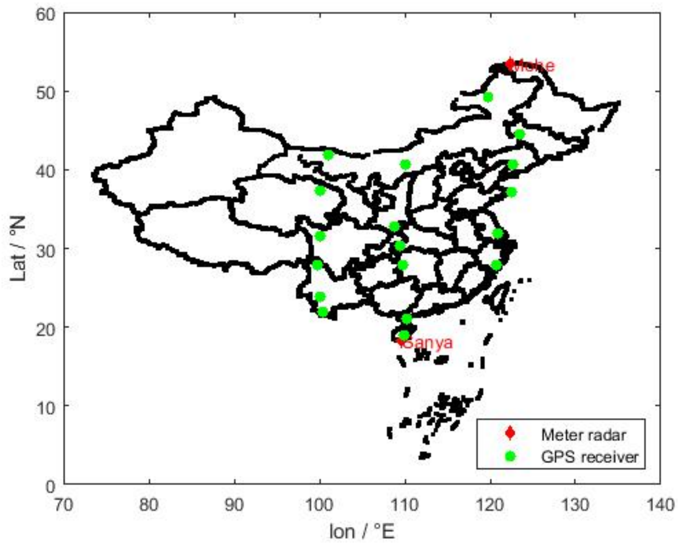

Figure1. The map of GPS receivers and Meteor radars.The green circles represent GPS receiver stations, and red diamonds represent the Meteor radars.

2.3 NCEP/NCAR Reanalysis data and Aura MLS data

The National Centers for Environmental Prediction(NCEP) and National Center for Atmospheric Research(NCAR) have cooperated in a project called reanalysis data that the temperature and wind are recovered from land surface, ship, rawinsonde, pilot balloon, aircraft, satellite, and other data (https://www.psl.noaa.gov//data/gridded/data.ncep.reanalysis.html). Daily averaged data are 2.5° × 2.5° grid for the whole world in latitude-longitude, 17 pressure levels from the Earth's surface up to 10 hPa. In this study, the stratospheric temperature at 10 hPa (approximately 30 km) at 60° N were used to obtain the temperature anomaly during 2013 SSW.

The Aura satellite was launched in July 2004. The angle between orbital plane and earth's equatorial plane is 82°, it rounds the earth 15 times a day. MLS(Microwave Limb Sounder, MLS) records atmospheric temperatures, density at different isobaric surfaces, 55 isobaric surfaces totally, corresponding height is 12~94km approximately (https://avdc.gsfc.nasa.gov/pub/data/satellite/Aura/MLS/V04/L2GP/Temperature/). In this paper, we used the MLS temperature data from December 1, 2012 to February 28, 2013 in the Northern Hemisphere to obtain the variations in temperature.

3. Results

3.1 2012-2013 SSW

Figure2a-d show the temperatures, wind, Kp and F10.7 from December 1, 2012 to February 28, 2013. The stratospheric warming began on the first day of 2013 (January 1, 2013) from ~60km and gradually downward to ~45km, it reached a secondary peak on the fourth day(January 4, 2013), the temperature peak occurred on the twelfth day(January 12, 2013) and the zonal wind shifted from west to east, then the temperature recovered slowly. The solar and geomagnetic conditions are indicated by F10.7 and Kp indices, respectively, both available at the website http://omniweb.gsfc.nasa.gov/form/dx1.html. The F10.7 index is in Solar Flux Unit (SFU = 10-22W/m2 /Hz). In this study, Kp≤4 is considered geomagnetically quiet. During the 2013 SSW period, geomagnetic activity was quiet, kp index was not more than 4. F10.7 began to increase from January 2013, reaching the peak on January 10, F10.7=168. It's obvious that the solar activity was high during the 2013 SSW.

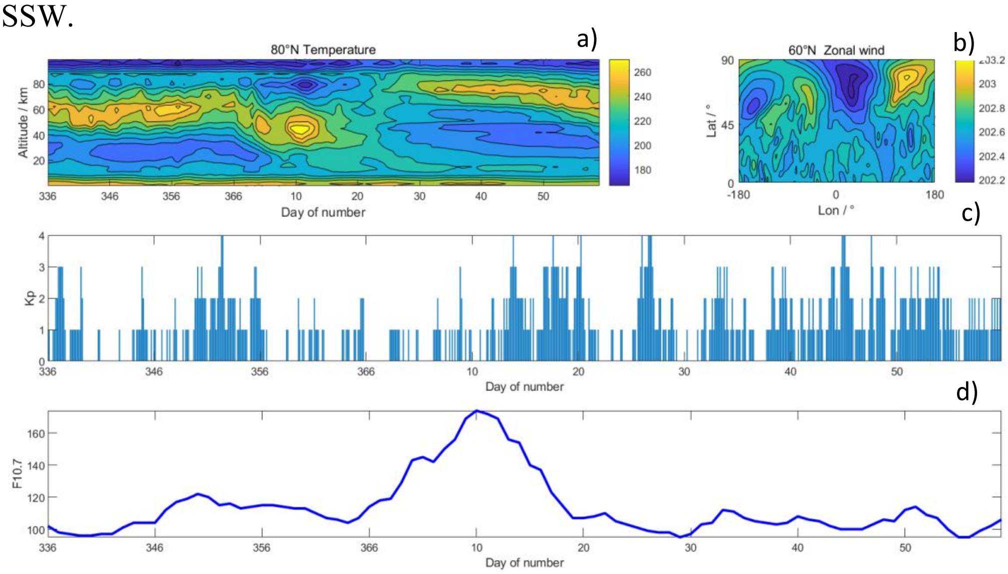

Figure2. The plots of temperatures, wind, F10.7 and Kp from December 1, 2012 to February 28, 2013. a) 80° N zonal averaged temperature. b) 60° N 10hpa zonal averaged wind on January 12. c) kp. d) F10.7.

3.2 Ionospheric response

To obtain the latitudinal and longitudinal differences in TEC during 2013 SSW , we chose eighteen GPS stations located along 100° E、110° E and 120° E covering 19.03° N to 49.21° N at latitude. The DTEC is the difference between the observed value(TEC) and the background value(TEC_{med}), which is used to extract the ionospheric disturbance. The background value TEC_{med} is the median value of TEC between December 1, 2012 and December 15, 2012.

Figure3 shows the variations of DTEC from January 1, 2013 to January 31, 2013, the two black dotted lines represent the peak time of the first temperature peak time (January 6) and the second peak time (January 12) , respectively. We can see that the TEC enhancement at ~01:00-08:00(UT) and decrease at ~8:00-12:00(UT) everyday at all stations along the chain 100° E during January 4 to 17, 2013. In other words, enhancement in TEC during morning and early afternoon, and decrease in the afternoon. This TEC semi-diurnal disturbance becomes more and more obvious with decrease in latitude until the YNZD station (latitude: 27.82N), then the semi-diurnal disturbance weaken gradually at YNLC(latitude, 23.87° N) and YNMH(latitude, 21.95° N). The maximum and minimum deviation in TEC are 175% and -58% along the chain 100° E. The variations of TEC on the chain 110°E are similar to the chain 100°E. The TEC semi-diurnal disturbance increase with decrease in latitude until HNMY(latitude, 27.88° N). Meanwhile, GDZJ (latitude, 21.16° N) and QION(latitude, 19.03° N) located in low latitude both weaken. The maximum and minimum deviation in TEC are 150% and -53% of the chain 110° E. On the chain 120° E，the variations of TEC are not clear at NMER（latitude, 49.21° N）and JLCL（latitude, 44.55° N）stations located at higher latitudes. The enhancement in TEC at morning is obvious from LNYK(latitude, 40.69° N) station and to the south until ZJWZ(latitude, 27.93° N) station, and the maximum deviation is 222%. But the decrease in TEC at afternoon is not clearly observed which is coincident with Chen(2019) along the chain 120° E .

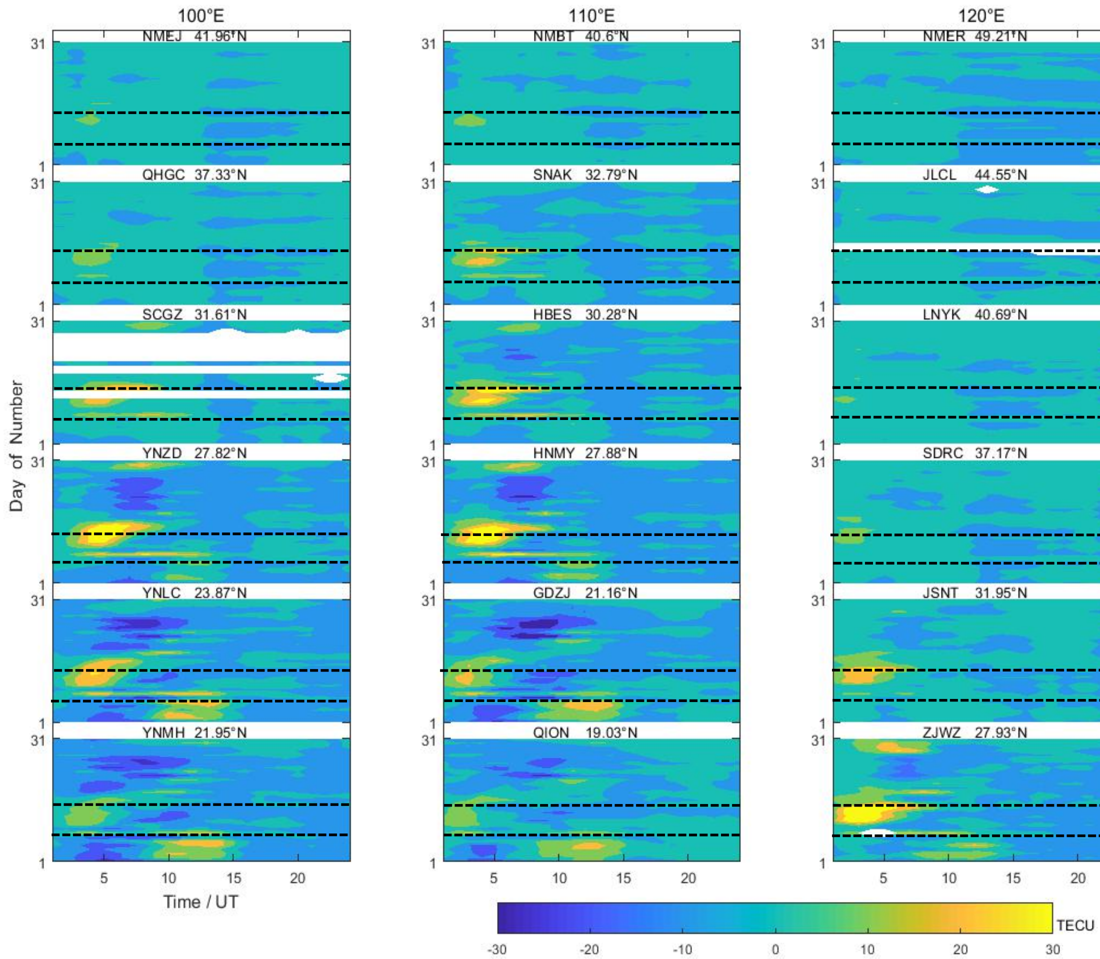

Figure3. variations of DTEC in TECu from January 1 to 31, 2013. The two black dotted lines represent the peak time of the first temperature peak (January 6) and the second peak time (January 12) , respectively.

From the above results, we can see that the TEC variations are not obvious when the latitude greater than 40° N. Inversely, the variations of TEC is obvious significantly with the decrease of latitude. The semi-diurnal variations of TEC in the form of morning enhancement and afternoon depletion are observed along the chain 100° E and 110°E and they increase with the decrease of latitude until ~27.82°N, then weaken significantly at YNLC, YNMH, GDZJ and QION stations located at latitudes less than 23.87° N. The TEC enhancement in the morning along the chain 120°E is evident, but weakening in the afternoon is not obvious. In a word, the TEC variations shows latitudinal dependence that the semi-diurnal variations in TEC takes equatorial ionization anomaly crest as the dividing line and weakens towards the two poles. Meanwhile, the longitudinal dependence in TEC variations is prominent during 2013 SSW. The TEC variations on the chain 100° E and 110° E are similar but different from the chain 120° E. The maximum deviation of TEC along the chain 120° E is larger than 100° E and 110° E, but the decrease at afternoon is not observed.

3.3 12-hour component of TEC

The TEC semi-diurnal disturbance is evident with latitude in sector 3.2. Figure 4 shows the wavelet power spectra of DTEC between January 1 to 31, 2013 to further analyze DTEC periodic variations. It can be seen that the DTEC have prominent 12-hour component period and the latitudinal characteristic is coincident with DTEC variations shown in Figure3. Hence, both DTEC and 12-hour component of DTEC take the equatorial ionization anomaly crest as the dividing line, decrease toward the two poles gradually, and disappear at higher latitude finally. As we all know that the tides occur mainly in MLT region and have maximum amplitudes in this region, they can affect the middle and low latitude ionosphere by modulating E-layer generators. It is assumed that the TEC semi-diurnal disturbance is caused by the semi-diurnal tide enhancement at the middle and low latitudes during 2013 SSW.

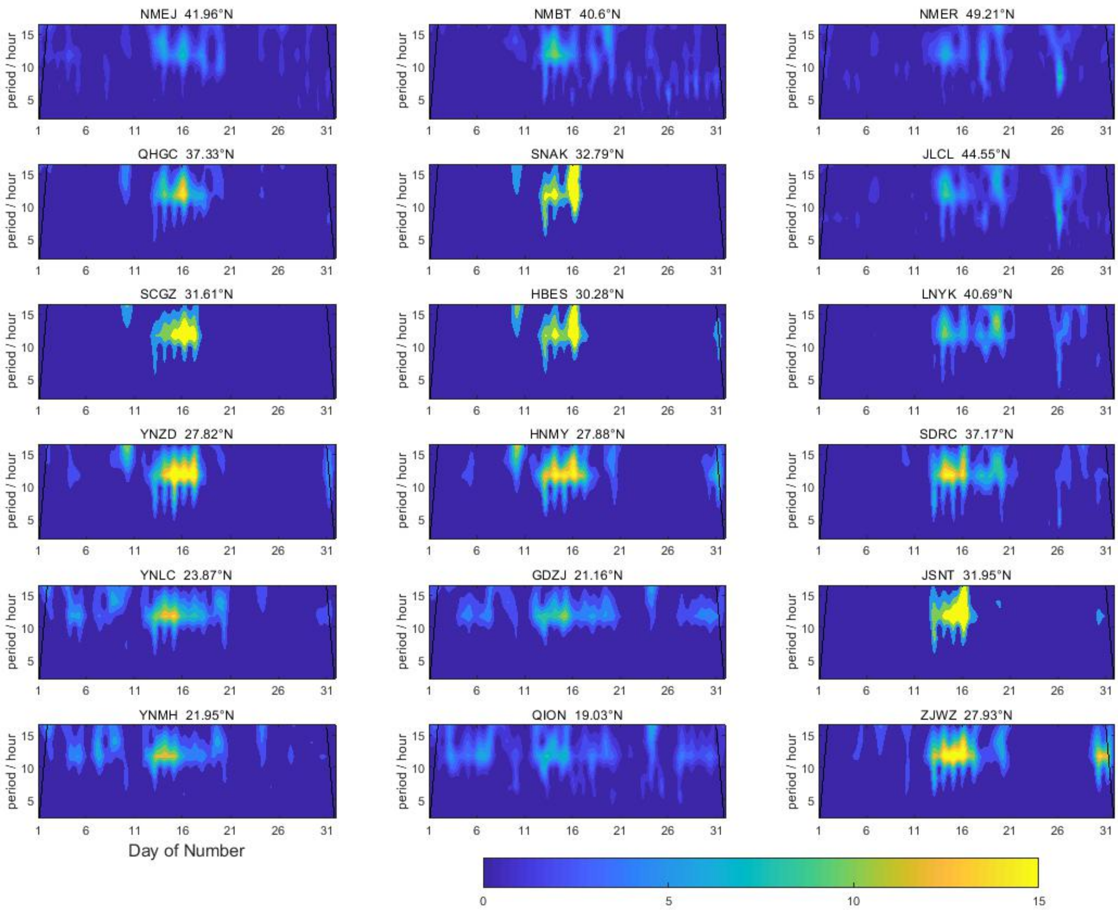

Figure4. Wavelet power spectra of DTEC between January 1 to 31, 2013.

3.4 Planetary wave variations in MLT

The zonal and meridional winds of Mohe and Sanya meteor radars were used to analyze the Planetary waves(PWs) variations in MLT region during the 2013 SSW at middle and low latitudes, respectively. The two radars can observe meridional and zonal winds at an altitude from 70km to 110km, with a altitude resolution of 2km and a time resolution of 1h. Considering the data quality, only the wind data at 92km, 96km and 100km heights were selected and processed the time resolution from 1h to 24h. Figure5-6 show the zonal and meridional winds wavelet power spectra at the 92km, 96km and 100km of Mohe and Sanya station, respectively. The quasi 10-Day planetary wave amplitudes are enhanced in zonal wind at Mohe all altitudes from December 20, 2012 to January 10, 2013 before warming, and the maximum amplitude is 7m/s at 92km. Quasi-16-day planetary wave amplitudes are enhanced in meridional wind from December 11, 2012 to January 27, 2013, and the maximum amplitude is 13.4m/s. Hence the quasi 16-day wave amplitude is higher than quasi 10-day wave amplitude at Mohe station. At Sanya, quasi-10-day planetary wave amplitudes are increased at all altitudes except for the 92km zonal wind, and the maximum amplitude is 7m/s. In general, the qusai-16-day waves are enhanced mainly at Mohe located at middle latitude and the qusai-10-day waves mainly at Sanya located at low latitude which are consistent with the variations of quasi-10-day and quasi-16-day planetary waves during SFW event in 2015 analyzed by Yu(2019).

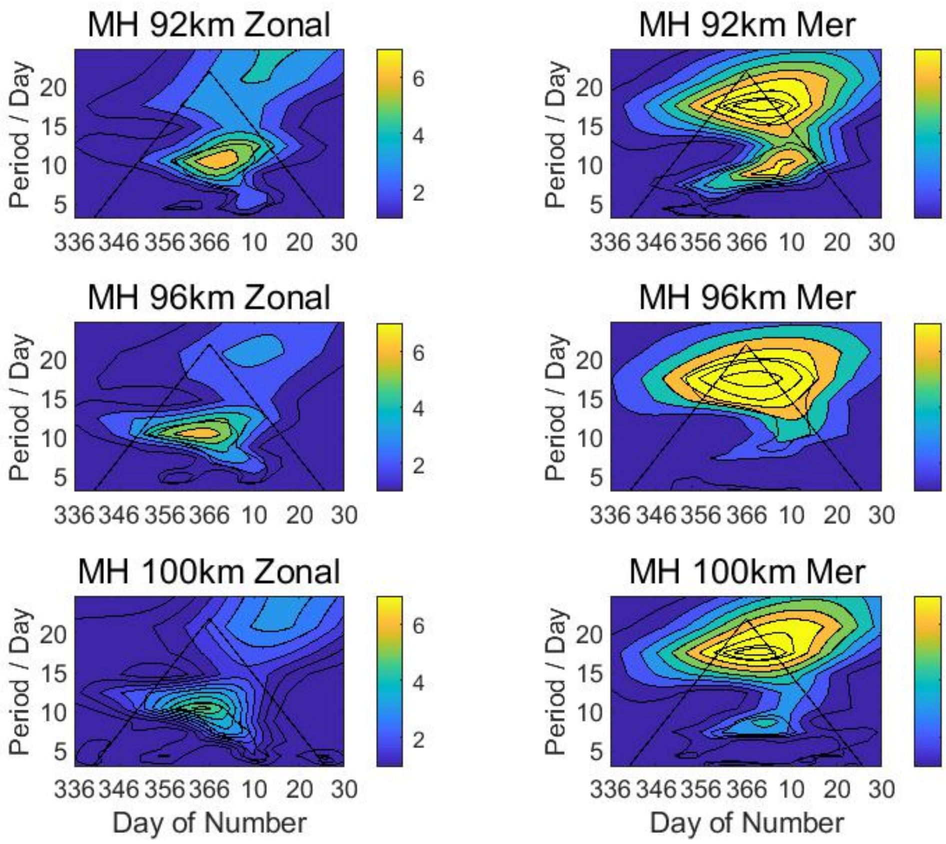

Figure5 Wavelet power spectra of zonal wind(left) and meridional wind(right) from December 1, 2012 to January 31, 2013 at Mohe station

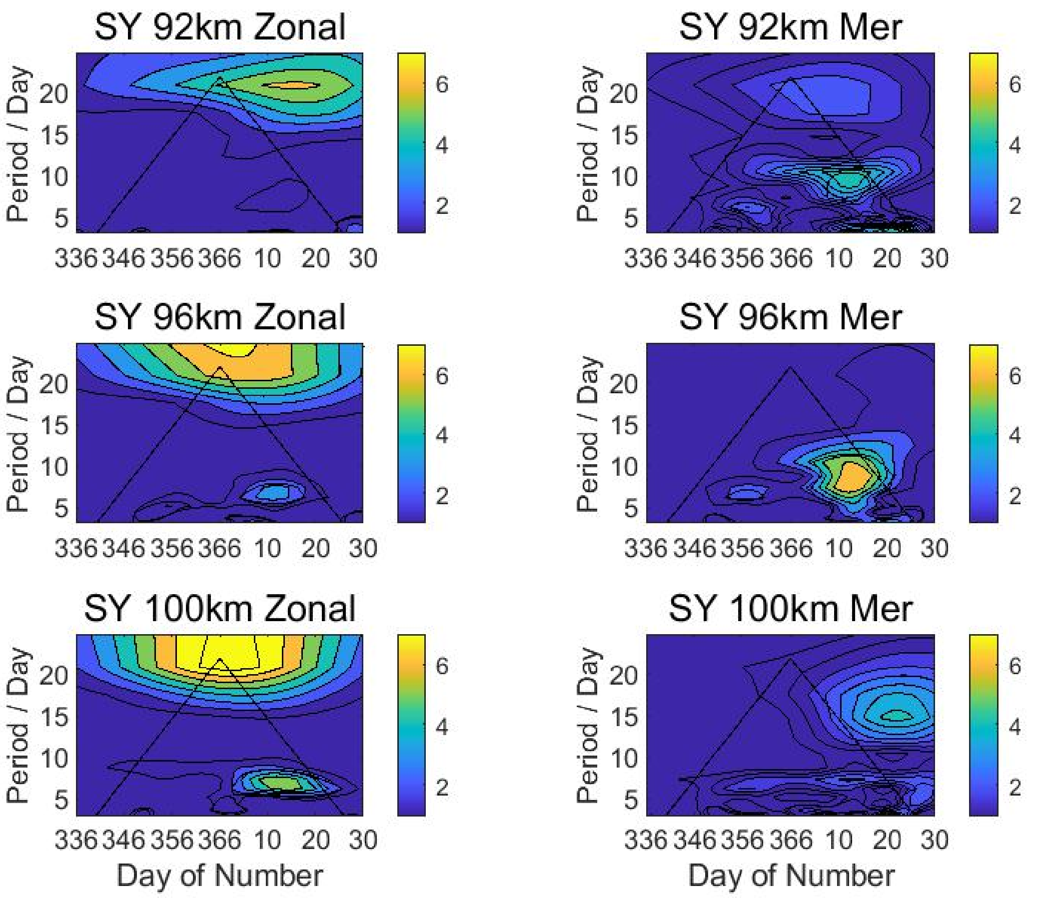

Figure6 Wavelet power spectra of zonal wind(left) and meridional wind(right) from December 1, 2012 to January 31, 2013 at Sanya station

4. Discussion

4.1 Latitudinal and Longitudinal Dependence

Previous reports and our results have shown that there are significant ionospheric perturbations along latitudes and longitudes during SSW events. In terms of the 2013 SSW, Figure 3-4 show the TEC response on the chain 100° E, 110° E and 120° E ranging from 19.03° N to 49.21° N at latitude. The semi-diurnal perturbation in TEC that morning enhancement and afternoon depletion were observed along the chain 100° E and 110° E. It takes the equatorial ionization anomaly crest as dividing line and decreases toward the two poles gradually, indicating that there exists a latitudinal dependence in ionospheric response to 2013 SSW. Liu (2013) showed the semi-diurnal variations in MLT region is prominent at low and middle latitudes but not at high latitudes, and the latitudinal variations is predicted in model simulations to provide thermospheric background is important to ionosphere. Meanwhile, the latitudinal dependence may be related to the the ionosphere characteristic that electron density is the largest in the equatorial ionization anomaly crest at geomagnetic latitude~±15° due to the equatorial fountain effect, and decreases toward the two poles gradually(Geetashree, 2020; Sumedha, 2021).

Figure 3 shows evident longitudinal dependence in ionosphere that the maximum deviation in TEC is 222% on the chain 120° E, which is more than 100° E and 110° E, but the afternoon depletion is weak. Geetashree (2020) studied the ionospheric response during 2013 SSW by TEC on the chain 10° E and 95° E, and discussed that the longitudinal differences might be attributed to the differential impact of the non-migrating tides and differences in the geomagnetic field elements between the two sectors. S. M. Liu (2019) studied that the semi-diurnal lunar tidal influence on low-latitudinal TEC tends to be more prominent in the American sector than in the East Asian sector during SSW events 2009-2018 and supported these differences due to the combined effect of tidal propagation and electrodynamic processes at these two sectors. In present work, the longitude difference is small between three chains, the geomagnetic field configuration is similar on different chains. Hence, the longitudinal ionospheric response in East Asia region during 2013 SSW may be attributed to differences in tidal influence on TEC by changing the [O/N2] ratio (Klimenko, 2013; Yasyukevich; 2018; Goncharenko, 2019).

4.2 Tide-PWs modulation

According to the above results and analysis, it is assumed that the ionosphere and lower atmosphere are probably coupled by the PWs forcing. The semi-diurnal tidal components of DTEC are extracted by harmonic fitting, with 2-day window and 1-day step, to analyze the coupling process between the semi-diurnal tidal components of TEC and PWs. Figure 7 shows the wavelet transform of semi-diurnal tidal components of DTEC at eighteen GPS stations. It indicates that the amplitudes of semi-diurnal tide at the latitude more than 23.87°N show obvious quasi 16-day wave-like oscillations along the chain 100°E and 110°E, while the quasi 10-day wave-like oscillations is weak relatively. But the quasi 10-day wave-like oscillations are clearly observed at YNMC, YNMH, GDZJ and QION stations located at low latitude. On the chain 120°E, the quasi 16-day wave-like oscillations are evident from LNYK (latitude: 40.69°N) to ZJWZ (latitude: 27.93°N), and they increase with the decrease of latitude. The results are consistent with the PWs fluctuations in the Mohe and Sanya in Figure5-6. According to the theory of PW-tidal modulation, the quasi 16-day PWs probably drive the TEC response by modulating tides at mid-latitude, and it might be attributed to the quasi-10 day planetary wave at low latitude.

The meridional and zonal winds are modulated by tides to change the electric field generated in layer E, which is mapped to layer F by magnetic field lines. This can drive the vertical drift of plasma and cause the ionospheric disturbance in the middle and low latitude (Liu, 2010). The ionospheric response, tide and planetary wave fluctuations in MLT region during the 2013 SSW further provide the coupling process of the ionosphere and MLT by tide-PWs modulation at middle and low latitudes.

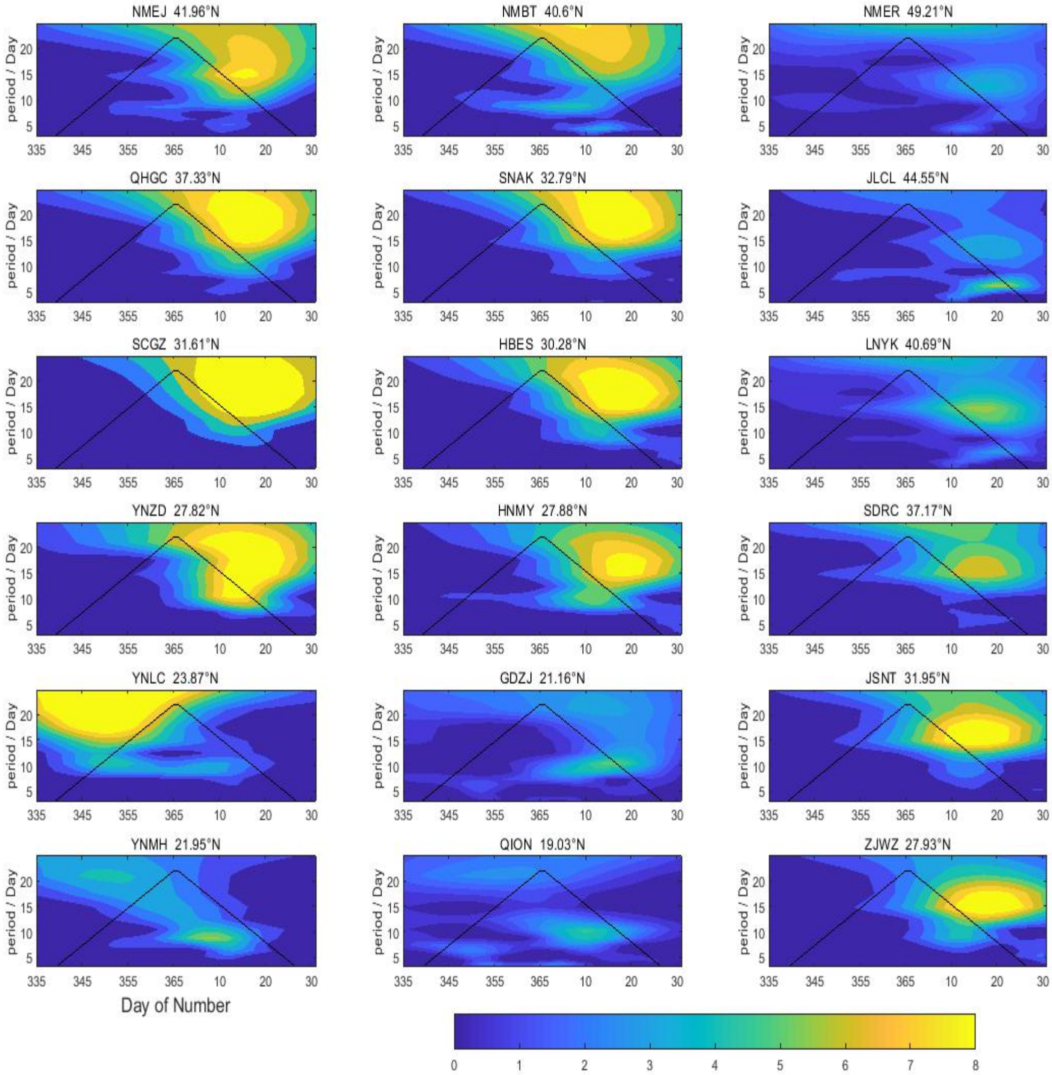

Figure7 Wavelet power spectra of DTEC semi-diurnal tidal component from December 1, 2012 to January 31, 2013 at all GPS TEC stations

5. conclusion

We use (a) TEC of three meridional chains with eighteen GPS stations at 100° E, 110° E and 120° E, ranging from 19.03° N to 49.21°N, and (b) zonal wind and meridional winds of the Mohe and Sanya Meteor Radars to observe the ionospheric response to the 2013 SSW at middle and low latitudes. Apart from some result generally consistent with the work of Chen(2019) and Geetashree(2020), there are some new results. Our main conclusions are summarized as follows:

1) The TEC variations are mainly manifested by the semi-diurnal variations of morning enhancement and afternoon depletion during 2013 SSW, which is consistent with the results of many scholars (Liu, 2019; Geetashree, 2020). Meanwhile, the TEC variations exhibited latitudinal and longitudinal dependence. This may be due to semi-diurnal tides variations in MLT region and ionospheric characteristic.

2) We use zonal wind and meridional winds of Mohe meteor radar and Sanya meteor radar to analyze PWs fluctuations in MLT region at middle and low latitudes. The quasi 16-day planetary waves in meridional wind at Mohe are amplified at an altitude of 92-100 km . The quasi 10-day planetary waves at Sanya are amplified at an altitude of 96-100 km. This indicates that the winds may be the main driver of the ionospheric anomalies during 2013 SSW.

3) The12h tidal components in TEC are amplified in the middle and low latitudes ionosphere during the 2013 SSW. The amplitudes of the 12 h components in TEC exhibit a period of 16 days at middle latitude and 10 days at low latitude. This suggests that the semi-diurnal tides are modulated by the 16 day planetary waves at middle latitude and by the 10 day planetary waves at low latitude, further providing the PW-tide interaction theory at middle and low latitudes over the East Asia region.

Acknowledgments

This work was supported by the National Key R&D Program of China (No.2020YFB0505603), the National Natural Science Foundation of China Program (No.41674081) and the Stable-Support Scientific Project of China Research Institute of Radiowave Propagation(No.A132011W16). We acknowledge the use of TEC data from Crustal Movement Observation Network of China(CMONC). The zonal wind and meridional wind of meteor radars are obtained from the World Data System (WDS)(http://wdc.geophys.cn/). The stratospheric parameters are downloaded from the National Centers for Environmental Prediction (NCEP) (http://www.cpc.ncep.noaa.gov) and Goddard Space Flight Center(GSFC)(https://avdc.gsfc.nasa.gov/). The Kp and F10.7 index data are obtained from the GSFC/SPDF OMNI Web interface (http://omniweb.gsfc.nasa.gov).

References

Boris G Shpynev.(2015), High-midlatitude ionosphere response to major stratospheric warming. Earth, Planets and Space (2015) 67:18 DOI 10.1186/s40623-015-0187-1.

Chen, G., C. Wu, S. Zhang, B. Ning, X. Huang, D. Zhong, H. Qi, J. Wang, and L. Huang (2016), Midlatitude ionospheric responses to the 2013 SSW under high solar activity, J. Geophys. Res. Space Physics, 121, 790–803, doi:10.1002/ 2015JA021980.

Dora Panchevan, Plamen Mukhtarov. Stratospheric warmings: The atmosphere–ionosphere coupling paradigm. Journal of Atmospheric and Solar-Terrestrial Physics 73 (2011) 1697–1702.

Laskar, F.I., and D. Pallamraju (2014), Does sudden stratospheric warming induce meridional circulation in the mesosphere thermosphere system?, J.Geophys.Res. Space Physics, 119, 10,133-10,143,doi:10.1002/2014JA020086.

Liu, H.-L., and A. D. Richmond (2013), Attribution of ionospheric vertical plasma drift perturbations to large-scale waves and the dependence on solar activity, J. Geophys. Res. Space Physics, 118, 2452–2465, doi:10.1002/jgra.50265.

Lin, J. T., Lin, C. H., Lin, C. Y., Pedatella, N. M., Rajesh, P. K., Matsuo, T., & Liu, J. Y. (2019). Revisiting the modulations of ionospheric solar and lunar migrating tides during the 2009 stratospheric sudden warming by using global ionosphere pecifification. Space Weather, 17, 767–777. https://doi.org/10.1029/2019SW002184

Li, N . Luan, X., Lei, J., O. S. B loaji, Owolabi, C., Chen, J., Xu, Z., Li. G, Ning, B(2020). variationss of mesospheric neutral winds and tides observed by a meteor radar chain over China during 2013 sudden stratospheric warming. JOURNAL OF GEOPHYSICAL RESEARCH: SPACE PHYSICS. https://doi.org/10.1029/2019JA027443.

LIU Kun, S H E N G Dongsheng, W A N G Feifei, Z H A N G Hongbo, LI Jianru. High precision algorithm for ionospheric V T E C based on single ground-based G N S S station (in Chinese). Chin. J. Space Sci., 2021, 41(3): 417-424. DOI: 10.11728/cjss2021.03.417

Luo, J., Gong, Y., Ma, Z., Zhang, S., Zhou, Q., Huang, C., et al. (2021). Study of the quasi 10-day waves in the MLT region during the 2018 February SSW by a meteor radar chain. Journal of Geophysical Research: Space Physics, 126, e2020JA028367. https://doi. org/10.1029/2020JA028367

J.R. Holton, H.-C. Tan, The inflfluence of the equatorial quasi-biennial oscillation on the global circulation at 50 mb. J. Atmos. Sci. 37, 2200–2208 (1980)

Geetashree Kakoti.,Bitap Raj Kalita et al(2020).Longitudinal and Interhemispheric ionospheric response to 2009 and 2013 SSW events in the African-European and Indian-East Asian sectors. American Geophysical Union. doi: 10.1029/2020JA028570

Guoqi Liu, Wengeng Huang.(2019). Ionospheric response to the 2018 sudden stratospheric warming event at mid- and low- latitude stations over China sector. American Geophysical Union doi: 10.1029/2019SW002160.

Jorge L. Chau, Larisa P. Goncharenko.(2012). Equatorial and Low Latitude Ionospheric Effects During Sudden Stratospheric Warming Events. Space Sci Rev (2012) 168:385 – 417. DOI 10.1007/s11214-011-9797-5.

Jonah, O. F., E. R. de Paula, E. A. Kherani, S. L. G. Dutra, and R. R. Paes(2014), Atmospheric and ionospheric response to sudden stratospheric warming of January 2013, J. Geophys. Res. Space Physics, 119,4973-4980,doi:10.1002/2013JA019491.

Fazlul I. Laskar.(2013) Investigations on vertical coupling of atmospheric regions using combined multiwavelength optical dayglow, magnetic, and radio measurements. JOURNAL OF GEOPHYSICAL RESEARCH: SPACE PHYSICS, VOL. 118, 4618–4627, doi:10.1002.

Fang, T.-W., T. Fuller-Rowell, H.Wang, R. Akmaev, and F.Wu(2014), Ionospheric response to sudden stratospheric warming events at low and high solar activity, J. Geophys. Res. Space Physics, 119,7858-7869, doi:10.1002/2014JA020142.

Korenkova, N.A., et al. Coupling between parameters of Es layer and planetary waves during SSW 2008, 2010. Adv. Space Res. (2015), http://dx.doi.org/10.1016/j.asr.2015.07.031.

Pancheva, D., and P. Mukhtarov (2011), Stratospheric warmings: The atmosphere-ionosphere coupling paradigm, J. Atmos. Sol. Terr. Phys., 73, 1697–1702, doi:10.1016/j.jastp.2011.03.006.

Sridharan, S. (2017), Solar and lunar tidal varibilities in GPS-TEC and geomagnetic field variationss: Seasonal as well as during the sudden stratospheric warming of 2010, J. Geophys. Res. Space Physics,122,4571-4587,doi:10.1002/2016JA023196.

Sumedha Gupta.(2021), Ionospheric Response to Sudden Stratospheric Warming Events Across Longitudes During Solar Cycle 24. Journal of Geophysical Research: Space Physics / Volume 126, Issue 10 / e2021JA029206

Sripathi, S., and A. Bhattacharyya (2012), Quiet time variability of the GPS TEC and EEJ strength over Indian region associated with major sudden stratospheric warming events during 2005/2006, J. Geophys. Res., 117, A05305, https://doi.org/10.1029/2011JA017103.

Maute, A., M. E. Hagan, V. Yudin, H. L. Liu, and E. Yizengaw(2015), Causes of the longitudinal differences in the equatorial vertical E×B drift during the 2013 SSW period as simulated by the TIME-GCM, J.Geophys. Res. Space Physics, 120,5117-5136, doi:10.1002/2015JA021126.

Matthias, V., Hoffmann, P., Manson, A., Meek, C., Stober, G., Brown, P., & Rapp, M. (2013). The impact of planetary waves on the latitudinal displacement of sudden stratospheric warmings. Annales Geophysicae, 31(8), 1397–1415. https://doi.org/10.5194/angeo-31-1397-2013

N.M. Pedatella, J.M. Forbes, Evidence for stratosphere sudden warming-ionosphere coupling due to vertically propagating tides. Geophys. Res. Lett. 37(11), 1–5 (2010a). doi:10.1029/2010GL043560

Pedatella, N. M., A. D. Richmond, A.Maute, and H.-L. Liu(2016).Impact of semi-diurnal tidal variability during SSWs on the mean state of the ionosphere and thermosphere, J. Geophys. Res. Space Physics, 121, 8077-8088, doi:10.1002/2016JA022910.

T. Matsuno, A dynamical model of the stratospheric sudden warming. J. Atmos. Sci. 28, 1479–1494 (1971)

Upadhayaya, A. K., and K. K. Mahajan (2013), Ionospheric F2 region: Variability and sudden stratospheric warmings, J. Geophys. Res. Space Physics, 118, 6736–6750, doi:10.1002/jgra.50570.

Wang F F, Chen J S，Xu T, et a1. 2015. Response of the sporadic-E layer to the stratospheric sudden warming in January 2009．Chinese J．Geophys. (in Chinese). 58(3): 721-728, doi: 10. 6038 / cjg20150302.

Yasunobu Miyoshi and Yosuke Yamazaki. Excitation mechanism of ionospheric 6-day oscillation during the 2019 September sudden stratospheric warming event. American Geophysical Union. doi:10.1029/2020JA028283.

Yamazaki, Y., & Matthias, V. (2019). Large-amplitude quasi-10 day waves in the middle atmosphere during final warmings. Journal of Geophysical Research: Atmospheres, 124, 9874–9892. https://doi.org/10.1029/2019JD030634

Yu, F. R., Huang, K. M., Zhang, S. D., Huang, C. M., Yi, F., Gong, Y., et al. (2019). Quasi 10- and 16-day wave activities observed through meteor radar and MST radar during stratospheric fifinal warming in 2015 spring. Journal of Geophysical Research: Atmospheres, 124, 6040–6056. https:// doi.org/10.1029/2019JD030630